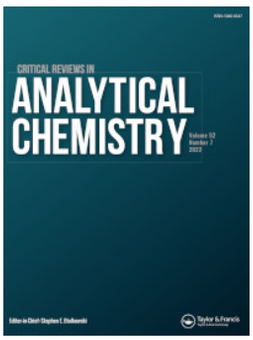

Taylor & Francis
Taylor & Francis Group

Critical Reviews in Analytical Chemistry

ISSN: (Print) (Online) Journal homepage: https://www.tandfonline.com/loi/batc20

Recent Advanced in MXene Research toward Biosensor Development

Md. Romzan Ali, Md. Sadek Bacchu, Md. Rashid Al-Mamun, Md. Ikram Hossain, Abdul Khaleque, Anowara Khatun, Dipto Debnath Ridoy, Mohamed Aly Saad Aly & Md. Zaved Hossain Khan

To cite this article: Md. Romzan Ali, Md. Sadek Bacchu, Md. Rashid Al-Mamun, Md. Ikram Hossain, Abdul Khaleque, Anowara Khatun, Dipto Debnath Ridoy, Mohamed Aly Saad Aly & Md. Zaved Hossain Khan (2022): Recent Advanced in MXene Research toward Biosensor Development, Critical Reviews in Analytical Chemistry, DOI: 10.1080/10408347.2022.2115286

To link to this article: https://doi.org/10.1080/10408347.2022.2115286

CRITICAL REVIEWS IN ANALYTICAL CHEMISTRY
https://doi.org/10.1080/10408347.2022.2115286

Recent Advanced in MXene Research toward Biosensor Development

Md. Romzan Ali[a,b], Md. Sadek Bacchu[a,b], Md. Rashid Al-Mamun[a,b], Md. Ikram Hossain[a,b], Abdul Khaleque[a,b], Anowara Khatun[a,b], Dipto Debnath Ridoy[a,b], Mohamed Aly Saad Aly[c], and Md. Zaved Hossain Khan[a,b]

[a]Department of Chemical Engineering, Jashore University of Science and Technology, Jashore, Bangladesh; [b]Laboratory of Nano-bio and Advanced Materials Engineering (NAME), Jashore University of Science and technology, Jashore, Bangladesh; [c]Department of New Biology, Daegu Gyeongbuk Institute of Science and Technology (DGIST), Daegu, South Korea

ABSTRACT

MXene is a rapidly emerging group of two-dimensional (2D) multifunctional nanomaterials, drawing huge attention from researchers of a broad scientific field. Reporting the synthesis of MXene was the following breakthrough in 2D materials following the discovery of graphene. MXene is considered the most recent developments of materials, including transition metal carbonitrides, nitrides, and carbides synthesized by etching or mechanical-based exfoliation of selective MAX phases. MXene has a plethora of prodigious properties such as unique interlayer spacing, high ion and electron transport, large surface area, excellent thermal and electrical conductivity, exceptional volumetric capacitance, thermal shock, and oxidation resistance, easily machinable and inherently hydrophilic, and biocompatibility. Owing to the abundance of tailorable surface function groups, these properties can be further enhanced by surface functionalization with covalent and non-covalent modifications via numerous surface functionalization methods. Therefore, MXene finds their way to a plethora of applications in numerous fields including catalysis, membrane separation, energy storage, sensing, and biomedicine. Here, the focus is on reviewing the structure, synthesis techniques, and functionalization methods of MXene. Furthermore, MXene-based detection platforms in different sensing applications are survived. Great attention is given to reviewing the applications of MXene in the detection of biomolecules, pathogenic bacteria and viruses, cancer biomarkers food contaminants and mycotoxins, and hazardous pollutants. Lastly, the future perspective of MXene-based biosensors as a next-generation diagnostics tool is discussed. Crucial visions are introduced for materials science and sensing communities to better route while investigating the potential of MXene for creating innovative detection mechanisms.

KEYWORDS

2D nanomaterials; biomolecules; biosensor; cancer biomarker; hazardous pollutant; MXene; mycotoxin; next-generation diagnostic tool; pathogenic bacteria and virus

1. Introduction

2D materials are crystalline materials known as single-layer materials. The interactions among atoms in 2D materials are stronger in the 2D plane (where electrons are free to move) than those in the thickness direction.[] Due to the prodigious atomic structure, high specific surface area, and novel electronic,[] optical, and mechanical[1] properties of 2D materials, leading to several promising applications, they attracted a great deal of the global attention. Furthermore, this attention has significantly increased since the mechanical exfoliation of graphene monolayer (single atom thick) that was first reported by Novoselov et al. in 2004.[] After the successful production of graphene single-layer and other 2D materials were formed by exfoliation.[2–4] Among 2D materials, MXene is the most advantageous materials due to high electrical conductivity which is important for enhancing the heterogeneous electron transfer rate. MXene is the 2D materials which is composed from carbide or nitride of transitional element where Ti and C in the case of $Ti_3C_2T_x$; and Ti, Mo, C in the case of double transition metal carbides; unlike graphene which consist of only one type of element; i.e., Carbon. The presence of multiple elements is advantageous in heterogeneous catalytic reaction due to their different affinities toward the target biomolecules. Similarly, MXene can be dispersed in common solvents such as water, ethanol, dimethylformamide, N-methyl2-pyrrolidone and others; with high stability from few days up to several weeks. The dispersion stability of MXene can be further improved by functionalization, as reported in a recent study.

Titanium Carbide (Ti_3C_2) is a recent 2D material well-known as MXene. It is an inorganic compound composed of thin layers of transition metals of carbonitrides, carbides, and nitrides and was first presented by Naguib et al. in 2011.[5] The formation of 2D Ti_3C_2 nanosheets, conical scrolls, and multilayer structures was first achieved by exfoliation of Ti_3AlC_2 in hydrofluoric acid (HF), that is, aluminum (Al) atoms are replaced by a hydroxyl (OH) as a result of reacting with HF followed by the breaking of the H-bonds, and finally the separation of the MXene single-layer at room temperature.[5] Ti_3AlC_2 is a member of a large class

CONTACT M. Z. H. Khan namelab.che.just@gmail.com Department of Chemical Engineering, Jashore University of Science and Technology, Jashore 7408, Bangladesh.

of materials that compose more than 150 families of polycrystalline ternary nitrides and carbides identified as the MAX phases.[6] Therefore, the introduction of Ti_3C_2 paved the road for the production of many other 2D materials. MAX phases have a common formulation of Mn + 1AXn, where n = 1, 2, or 3, M is a transition metal, A is an 'A group' (mainly 13 and 14) element such as aluminum or silicon, and X is either carbon (C) or nitrogen (N).[7,9] Normally, MXene are produced by etching or exfoliation from a 3D precursor of the MAX phase compound. To obtain two-dimensional layers of MXene, a single layer from the MAX phase material is selectively removed by a chemical reaction called intercalation followed by delamination.[10]

MXenes possess remarkable properties such as biocompatibility,[11] large surface area, unique interlayer spacing, high ion and electron transport, excellent conductivity (both thermal and electrical), thermal shock and oxidation resistance, exceptional volumetric capacitance, easily machinable and inherently hydrophilic.[12] Owing to the abundance of tailorable function groups presence on their surface such as oxygen, fluorine, hydroxyl, and chloride, these properties can be further enhanced by surface functionalization with covalent and non-covalent modifications via numerous surface functionalization methods such as self-assembly,[13] in situ polymerization,[14] electrostatic assembly,[15] hydrothermal approach[16] and heat and milling treatment.[17] Therefore, MXene find their way to a plethora of applications in numerous fields such as catalysis,[18] membrane separation,[19] energy storage,[20] sensing,[21] and biomedicine.[22]

Despite their brief journey, MXene have shown promising potential as highly sensitive and selective detection tools for broad detection applications.[23] Large surface area, biocompatibility, drug loading capacity, and nontoxicity are among the overwhelming number of outstanding properties of MXene that paved the road for their use in advanced sensing applications.[24,25] The literature revealed that MXene are promising candidates for the immobilization of protein and enzyme, promoting low detection limits, superior selectivity, and sensitivity.[26] Furthermore, it was reported that MXene-based electrochemical sensors offer outstanding detection characteristics when biological receptors are immobilized on the MXene surface-modified electrodes.[27]

The antibacterial properties of MXene have been investigated and reported.[28] Rasool et al. described the antibacterial activity of two-dimension MXene ($Ti_3C_2T_x$) suspension.[29] They found that single and layered $Ti_3C_2T_x$ flakes in colloidal solution displayed a greater antimicrobial property on both E. coli and B. subtilis when compared with a well-known antibacterial agent (graphene oxide). Recently, the sensing capabilities of MXenes against CoVID-19 were reviewed and reported.[30] Moreover, Li et al. investigated the sensing capabilities of MXene against the different concentrations of antigens from both 2019-nCoV and influenza virus by developing a low-cost MXene-graphene field-effect transistor (FET) detector integrated into a microfluidic channel, receiving viruses in solution.[31] The developed platform displayed a low detection limit, outstanding sensitivity, rapid-responding performance, and a high signal-to-viral load ratio.

Among the broad applications of MXenes, cancer diagnosis via detecting cancer biomarkers by using MXene-based sensors has drawn a great deal of the attention of the scientific community. Lately, the synthesis of amino silane-functionalized MXene (Ti_3C_2) nanosheets by minimally intensive layer delamination method was investigated and reported.[32] The developed label-free ultrasensitive electrochemical biosensor was used for cancer cell detection applications. The amino group functionalized MXene offered a reliable base for cancer bio-receptor covalent immobilization toward the detection of cancer biomarkers (carcinoembryonic antigen) found in numerous kinds of cancers for instance colorectal, lung, ovarian, pancreatic, breast, and liver cancers. Furthermore, Sadiq et al. reported MXene (Ti_3C_2)-based biosensor to accurately detect PGE2 and 8-HOA in A549 lung cancer cells with outstanding selectively, high-to-noise ratio, and exceptional sensitivity.[33]

MXene-based electrochemical biosensor as tools to sense food contaminants, mycotoxins, toxic elements, hazardous pollutants, and environmental pollutants were studied and reported.[34,35] The developed electrochemical sensor proved to be a promising sensing system for environmental and food safety applications and further displayed excellent selectivity, stability, reproducibility, and repeatability. Furthermore, MXene-based aptasensor for detecting the different types of mycotoxins were studied and reported.[36]

In the current work, we focus on examining the structure, synthesis methods, and functionalization techniques of MXene. Moreover, MXene-based detection platforms in a wide range of sensing applications are survived. Furthermore, the application of MXenes in detecting biomolecules, pathogenic bacteria and viruses, cancer biomarkers, food contaminants, and mycotoxins is reviewed in detail. Finally, perspectives for the future of MXene-based biosensors as a next-generation diagnostics tool are discussed.

2. Synthesis and functionalization of MXene

Currently, there are more than seventy distinct MAX phases were generated and over twenty MXenes were produced. The fundamental idea of MXene production is to eliminate the element 'A' from MAX phases where 'M' is an early transition metal, 'A' is an element from 'group A' (generally group 13 and 14), and 'X' referrers to either C or N.[12,37]

Various etching methods were developed for MXene synthesis. M. Naguib and coworkers first developed the hydrogen fluoride (HF) etching method for the synthesis of MXene from the MAX phase. In a Ti_3AlC_2 MAX phase, Al was extracted by HF, and $Ti_3C_2T_x$ (where T represents a surface functional group -OH, -O, -F), MXene, was synthesized.[38] M. Naguib and coworkers also synthesized Ti_3AlCN, $(Ti_{0.5}, Nb0.5)_2AlC$, Ta_4AlC_3, $(V_{0.5}, Cr_{0.5})_3AlC_2$, and Ti_2AlC following the same process.[12]

The Traditional HF etching method suffers from a major disadvantage; a strong acid solution causes surface defects and lowers the yield.[39] To avoid this, Ghidiu and coworkers developed an improved method by using a mixture of a milder acid solution of HCl and fluoride salt (LiF, KF, NaF, CaF).[40] Furthermore, A mixture of FeF_3/HCl was introduced by X. Wang and coworkers.[41] More etching techniques were developed and offered milder etching conditions, shorter sonication time, higher exfoliation yield, fewer flaws, and improved surface quality.[37,42] Halim and coworkers demonstrated a method using NH_4HF_2 as an etchant for Titanium Carbide based MXene (Ti_3C_2).[43] Additional bifluoride salts ($NaHF_2$, KHF_2) were suggested by A. Feng and coworkers for the synthesis of titanium carbide-based MXene.[5]

For nitride-based MXene, the fluoride-based etching method was not effective, therefore, P. Urbankowski and coworkers introduced a new etching method by using LiF, KF, and NaF (LiF:NaF:KF = 29:12:59 weight ratio) molten salt to remove Al from the MAX phase.[44] They produced titanium nitride ($Ti_4N_3T_x$) based MXene from the titanium aluminum nitride (Ti_4AlN_3) MAX phase. S. Yang and coworkers established a fluorine-free electrochemical method for titanium aluminum carbide-based (Ti_3AlC_2 MAX phase) with a 90% yield.[45] They used NH_4Cl and TMASO (tetramethylammonium hydroxide) as an electrolyte acting as an etchant. Aside from the acid-based etching, a method using alkaline solution (NaOH) was established by T. Li and coworkers for MXene synthesis.[46] J. Xuan and coworkers also used organic alkaline solution (TMASO) as etchant.[47] Alhabeb and coworkers developed a new process for the large production of MXene from the silicon base MAX phase (Ti_3SiC_2).[48] They used a mixture of HF and oxidant (H_2O_2, persulfate, permanganate, HNO_3, O_3) for removing silicon to produce MXene.

MXene nanosheets offer a large surface area with an abundance of functional groups (such as oxygen, fluorine, hydroxyl, and chloride) present on their surface, allowing easier surface functionalization to modify their conductive properties and further bind to biological molecules.[23,49] Owing to the presence of hydroxyl group on MXene surface, simple, tunable, and robust surface modification using silane chemistry made possible allowing the deposition of a large range of functional groups for further immobilization of biomolecules.[50] The immobilization capacity and sensing properties of MXene can be enhanced after successful functionalization. The negatively charged MXene is functionalized by positively charged molecules.[51] The surface functionalization and modification can be done by following physical absorption and electrostatic attraction improving the bioreceptor absorption capability of MXene. A. Koyappayil and his coworkers developed β-hydroxybutyrate dehydrogenase linked MXene nanocomposite for sensing β-hydroxybutyrate.[52] To prepare the nanocomposite, MXene was mixed with the enzyme and functionalized by using bovine albumin serum (BSA), NAD^+, and glutaraldehyde (GA). The surface of MXene has been modified DNA, or oligonucleotide such as aptamer, antibody by functionalizing MXene with different crosslinker to attach thiol, amino or carboxylic group on MXene.[53] Covalent immobilization, physical adsorption, and electrochemical adsorption are the most commonly used technique to immobilize bio-receptors on the surface of MXene in which covalent immobilization is more preferable for attachment of DNA or nucleotide on MXene.

3. Application of MXene-based biosensor

MXene is one of the latest explored advanced materials applied in sensing and biosensing area after extensive utilization of different 2D materials such as carbon-based materials, metal oxide materials and other layered materials. MXene is used in biosensor fabrication to amplify the signal (electrical or Optical) of biosensor due to its prominent features such as extraordinary surface chemistry, excellent conducting properties, biocompatibility, and easy functionalization and immobilization of biological receptors. Numerous MXene based biosensing approaches have been developed for sensing pathogenic bacteria and viruses, biomolecules, food contaminants, infectious diseases biomarkers, environmental hazardous organic pollutant and pesticides providing electrical or optical signal. Based on the electrical or optical signal the MXene based biosensors are classified into electrochemical or optical biosensor. In electrochemical biosensor, the targeted substances can be detected with presence of target specific bioreceptor such as DNA, RNA, Aptamers, Nucleic acids, Proteins, Enzymes, etc. The MXene based electrochemical biosensor can be designed by immobilization the selective bioreceptor. The bioreceptors produce electrochemical signal by interacting target molecules and MXene enhance the signal into greater magnitude. On the hand, the optical signal (change in color, reflective index, light intensity) is found after interaction of bioreceptor and specific targets is amplified by MXene due to its unique optical properties in MXene based optical biosensor.

In this section, application of MXene in development of electrochemical or optical biosensor for detecting biomolecules, pathogenic bacteria and viruses, food mycotoxins, cancer biomarkers, and environmental hazardous pollutants.

3.1. Sensing biomolecules

Biomolecules have an important role in human routine activities and disease resistance, particularly for tiny biomolecules with high reducibility's, such as glucose, cholesterol, ascorbic acid, neurotransmitter, glutamate, dopamine, and uric acid.[54] They serve a crucial function in the maintenance of human health. As a result, it is critical to be able to identify these biomolecules simply and quickly to monitor human health.[55] Traditional methods for monitoring biomolecules include high-performance liquid chromatography,[56] spectrometry,[58] and colorimetry.[59] However, these methods have some drawbacks such as being time-consuming, requiring expensive reagents, calling for complex extraction procedures, and demanding intensive training.[60]

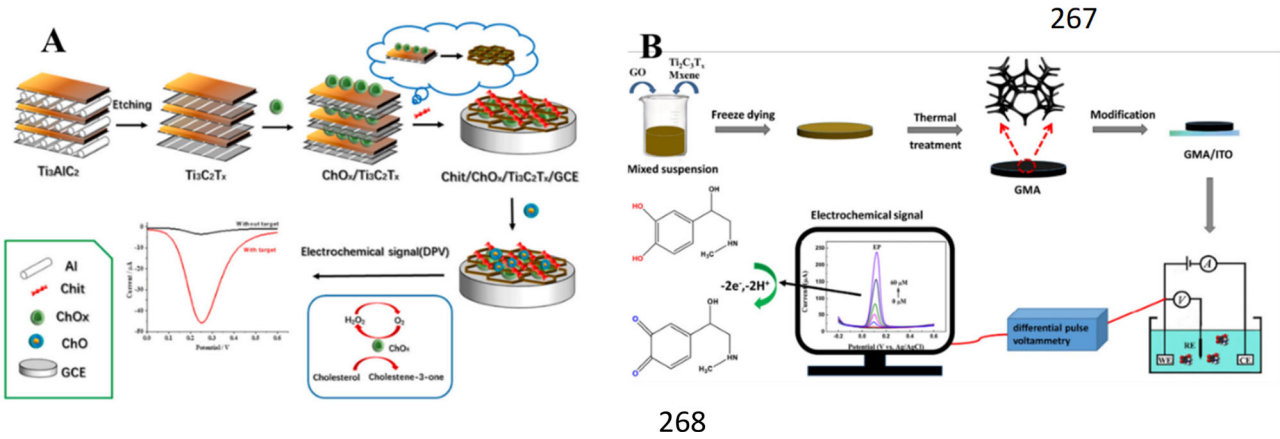

Figure 1. (A) The fabrication process of Chit/ChOx/$Ti_3C_2T_x$ modified glass carbon electrode and a proposed reaction mechanism of cholesterol at the surface of the functionalized glass carbon electrode. Reprinted from [51] with permission: Copyright © 2021 Elsevier B.V. (B) Illustration of preparing GMA/ITO modified electrode and the electrochemical sensing of EP. Reprinted from [67] with authorization: Copyright © 201Elsevier B.V.

Recently, biosensors become favorable for detecting biomolecules due to their unique characteristics such as high selectivity, sensitivity, accuracy, compatibility and stability, low cost, and less time-consuming.[61–64] To enhance the performance of biosensors, different metals, metal oxides, carbides, nitrites nanoparticles, and structural nanosheets are integrated into the fabrication of biosensors. Among these nanomaterials, MXene provides several effective surface sites suitable for the immobilization of bioreceptor enhancing the selectivity, stability, sensitivity, and accuracy of the biosensor.[23]

Rakhi and her team introduced Au/MXene composites-based biosensing system for detecting glucose.[65] In that work, the biosensor was fabricated by incorporating glucose oxidase (GDx) on the surface of an electrode functionalized with Nafion solubilized Au/MXene nanocomposite. The developed biosensor provided a linear amperometric response with a glucose concentration ranging from 0.1–18 mM and a LOD of 5.9 μM. The selectivity of the biosensor was confirmed by examining the common electroactive interfering compound such as Dopamine, Uric acid, and Ascorbic acid. In another work, Sun et al. proposed a sensitive electrochemiluminescence (ECL) biosensor for monitoring glucose in fruits, human serum, and sweat samples.[66] To construct the biosensing platform, GDx was immobilized on the surface of the glycine functionalized nanoplatform of TiO_2 nanowires on Ti_3C_2 MXene. The ECL biosensor can detect glucose in a wide concentration range of 12 mM–20 nM with a LOD of 1.2 nM. Monitoring cholesterol levels is essential for human health because unstable cholesterol levels cause serious health problems. To explore simple, sensitive, effective tools for monitoring cholesterol, T. Xia et al., developed a $Ti_3C_2T_x$ MXene-based enzymatic electrochemical biosensing platform for the detection of cholesterol.[51] This research team fabricated the biosensor by immobilizing the cholesterol oxidase (ChOx) enzyme on the electrode surface by using chitosan and MXene as supporting materials for attaching the enzyme as schematically shown in Figure 1(A). The developed ultrasensitive biosensor provided an excellent linear relationship in a concentration range of 0.3–4.5 nM with a LOD of 0.11 nM. To develop MXene based biosensor to detect neurotransmitters, F. Shahzad et al., proposed an MXene-based electrochemical biosensor for sensing dopamine (DA).[68] The proposed biosensor offered a wide window for the detection of DA (0.015–10 µM) with a LOD of 3 nM. Additionally, Li et al., introduced an electrochemical biosensing platform for sensing another neurotransmitter, epinephrine (EP).[67] To fabricate the biosensor, $Ti_3C_2T_x$ MXene and reduced graphene oxide (rGO) were mixed to form MXene-rGO (GMA), and next GMA was transferred on the surface of ITO as shown in Figure 1(B). The biosensor provided a linear current response with an EP concentration range of 1–60 μM and LOD of 3.5 nM. Recently, A. Koyappayil et al. presented β-hydroxybutyrate dehydrogenase decorated MXene nanosheet-based biosensor for the identification of β-hydroxybutyrate.[52] The proposed biosensor provided a wide range of linearity (0.36 to 17.9 mM) with a LOD of 45 μM. A list of MXene-based biosensor developed for sensing biomolecules along with a comparison of their analytical performance is summarized in Table 1.

3.2. Sensing pathogenic bacteria and viruses

Pathogenic bacteria and viruses are the main sources of pandemic diseases and human death worldwide.[72,73] Rapid and early-stage identification of viruses and pathogenic bacteria is essential for selecting proper diagnosis and reducing the complexities of diseases, managing and controlling the spreading efficiency of the bacteria and viruses.[74] Recently, COVID-19 provided a valuable example showing the essence of early-stage detection in controlling the spread of infection disease.[75] Thus, researchers are actively working on developing an effective diagnostic tool for the rapid and early detection of viruses and pathogenic bacteria.[76] Diverse technologies are applied to identify bacteria and viruses such as the bacterial culture method,[77] enzyme-linked immunosorbent assay,[78] real-time PCR, and real-time RT-PCR.[,79] But these methods have disadvantages such as being time-consuming, requiring expensive reagents, calling for complex extraction procedures, and demanding extensive training.[60] Recently, biosensors become favorable for detecting

Table 1. List of MXene-based biosensor developed for sensing biomolecules.

Sensing matrix	Bio-recognition element	Biosensing technique	Target analyte	Sensing performance			Ref.
				Linear range	LOD	Sensitivity	
GODx/Au/MXene/Nafion/GCE	Enzyme	Electrochemical biosensor	Glucose	0.1 to 18 mM	2.6 μM	4.2 μAmM^{-1} cm^{-2}	[65]
GODx/glycine-TiO_2-Ti_3C_2/GCE	Enzyme	Electrochemical biosensor	Glucose	20 nM to 12 mM	. nM	–	[66]
Chit/ChOx/$Ti_3C_2T_x$/GCE	Enzyme	Electrochemical biosensor	Cholesterol	0.3 to 4.5 nM	0.12 nM	132.66 μA nM^{-1} cm^{-2}	[51]
Ti_3C_2/DNA/Pd/Pt@GCE	DNA	Electrochemical biosensor	DA	0.2 to 1000 μM	27 nM	–	[69]
$Ti_3C_2T_x$/GCE sensor	–	Electrochemical biosensor	DA	0.015 to 10 µM	1 nM	–	[68]
GMA/ITO	–	Electrochemical biosensor	EP	1 to 60 µM	1.2 nM	3.74 μA. μM^{-1}·cm^{-2}	[67]
Au-PCB/Ru/MXene-β-HBD-NAD$^+$-GA-BSA	Enzyme	Electrochemical biosensor	β-hydroxybutyrate	0.36 to 17.9 mM	42 µM	0.480 μA mM^{-1} cm^{-2}	[52]
GCE/PtNP@MXene-$Ti_3C_2T_x$/Chi/GluOx/Chi	Enzyme	Electrochemical biosensor	L-glutamate	10–110 μM	0.45 μM	1.5906 nA/(μmol/L)	[70]
MIP/d-Ti_3C_2T/MWCNTs/GCE	–	Electrochemical biosensor	Amyloid-β protein b	0.36 to 17.9 mM	47 μM	–	[52]
LOx/Pt/PANI/MXene	Enzyme	Electrochemical biosensor	Lactate	0.005 to 17.9 mM	2 μM	–	[71]

microorganisms owing to their unique characteristics such as high accuracy, sensitivity, selectivity, compatibility and stability, low cost, and less time-consuming.[63,64,80–82] Several receptors are used to fabricate biosensors for the detection of microorganisms such as DNA, aptamer, antigen-antibody complexes, enzymes, and proteins providing the output in the form of electrical or optical signals. Due to the outstanding electrical and optical properties of MXene, it is a suitable candidate for biosensing applications including sensing pathogenic bacteria and viruses.[83] MXene is an effective material for developing biosensors due to its exclusive properties of high electric conductivity, easier incorporation ability of discrete functional groups, and excellent ion-intercalation characteristic, thus becoming suitable for the fabrication of biosensing platforms. MXene provides numerous effective sites for the immobilization of bioreceptor on its surface enhancing the selectivity, stability, sensitivity, and accuracy of the biosensor.[23] Figure 2 shows the fabrication principle of MXene-based biosensor for viruses and pathogenic bacteria.

As an effort toward developing of MXene based biosensor for the identification of viruses, Chen and his research team recently introduced a DNA functionalized MXene-based chemoresistive biosensor for selective and quick sensing of the nucleocapsid gene of SER-CoV-2 (SER-CoV-2 N gene) (W. Y. Chen et al. 2022). In that work, the biosensing platform was fabricated by noncovalent adsorption of the probe DNA molecule and 2D $Ti_3C_2T_x$ MXene. In that sensing platform, the conductance of the sensing channel was increased after hybridization of complementary SER-CoV-2 N gene with probe ssDNA on the surface of MXene, however, no response was found for non-complementary targets (SER-CoV-1 N gene and MER-CoV N gene) suggesting high selectivity of the biosensor. Figure 3(A) shows the detection principle of the SER-CoV-2 N gene by using the sensing platform of DNA functionalized MXene. The biosensor showed LOD below 10^5 copies/ml in saliva similar to the result of RT-PCR.

Most recently, an aptamer-based SPR biosensing platform was constructed to detect the SER-CoV-2 N gene.[85] To fabricate the biosensor, N-gene-targeted N58 aptamer was immobilized on thiol-modified niobium carbide-based MXene quantum dots. The biosensor displayed a linear relationship for the detected signal virus with the logarithm value of N-gene concentration of 5×10^{-2}–100 ng m/L with LOD of 4.9 pg m/L. The electrical conductivity of MXene improves when combined with different metal-organic frameworks (MOF). Lately, Y. Wang introduced an imidazole metal-organic framework (ZIF-8) combined with $Ti_3C_2T_x$ MXene-based electrochemical electrochemiluminescence (ECL) biosensor for screening human immunodeficiency virus-1 (HIV-1).[86] To fabricate the biosensor, a particular aptamer was attached to the surface of $Ti_3C_2T_x$/ZIF-8/GCE, and further ssDNA functionalized conductive carbon black along with magnetic nanoparticles (MNPs) were immobilized on the surface of the aptamer modified electrode. The ECL signal was risen by enhancing the concentration of HIV-1 protein while being linear in the concentration range of 1 fM–1 nM with a LOD of 0.3 fM. X. Peng et al., explored a fluorescent sensor for monitoring human papilloma virus-18 (HPV-18) infection in a real sample.[87] The transducer of the sensing platform was fabricated by the combination of ultrathin MXene nanosheets, dye-labeled ssDNA probe, and exonuclease III (Exo III). The pioneer research team demonstrated the ability of the proposed sensing platform in detecting HPV picomolar levels and further demonstrated a linear response at HPV ssDNA concentration range of 0.5 nM–50 nM.

Recently, a wide group of scientists become interested in fabricating MXene-based diagnostic tools for monitoring pathogenic bacteria. Zhang et al. applied for the first time the MXene-based biosensing strategy in the determination

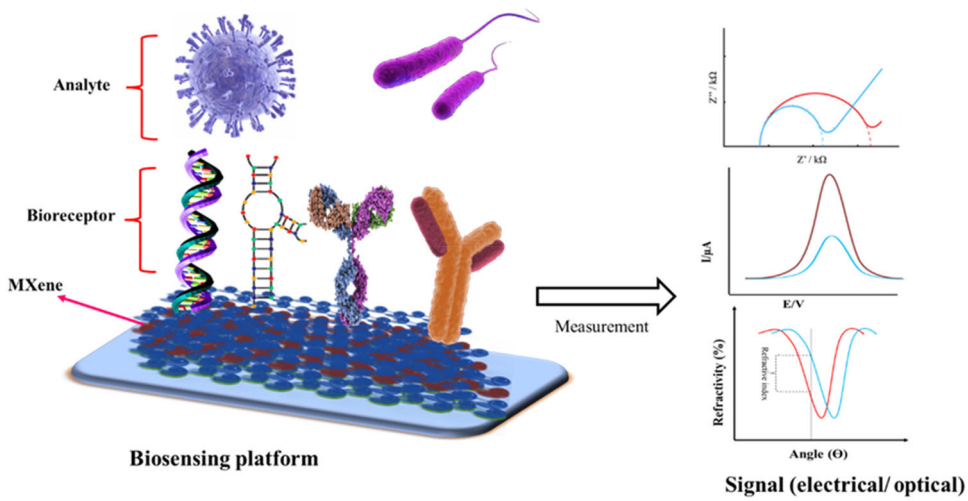

Figure 2. Systematic sensing mechanism of MXene-based biosensor for detection of viruses and pathogenic bacteria.

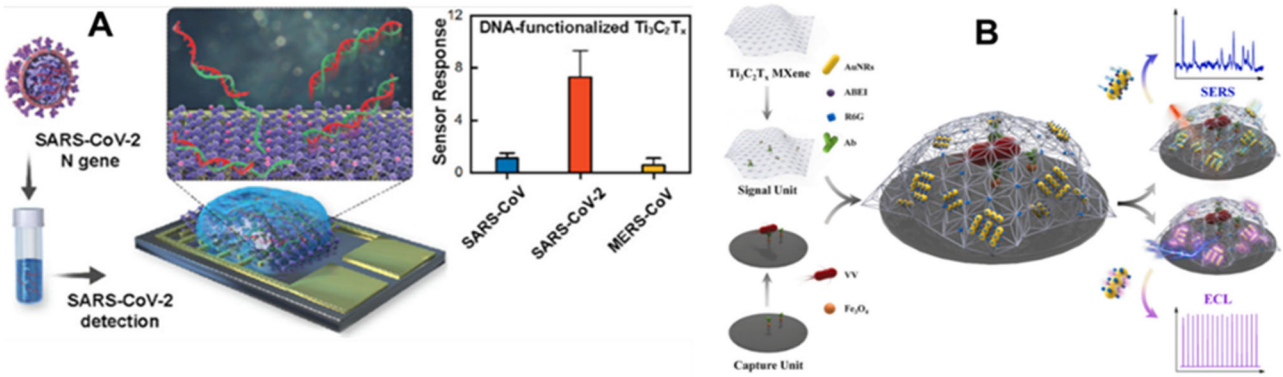

Figure 3. (A) Schematics illustrating the operation of ssDNA/$Ti_3C_2T_x$ detectors for the sensing Covid-19 nucleocapsid (N) gene. Reprinted from (W. Y. Chen et al. 2022) with authorization: copyright © American Chemical Society; (B) Schematic diagram of the dual-mode ECL/SERS immunosensor for VV. Reprinted from [84] with authorization: Copyright © 2021 Elsevier B.V.

of *Mycobacterium tuberculosis* (*M. tuberculosis*).[88] To construct the biosensor, peptide nucleic acid (PNA) was used as a capture probe of specific targets, and zirconium-linked Ti_3C_2 MXene was used as a signal enhancer. The *M. tuberculosis-specific* target biomarker hybridized with PNA was immobilized on the gold surface of the electrode and the conductance of the modified electrode was enhanced after the interaction of conductive MXene with the target biomarkers. The developed biosensor showed high discrimination ability in the detection of *Escherichia coli* (*E. coli*), *Pseudomonas aeruginosa (P. aeruginosa), M. tuberculosis*, *Mycobacterium smegmatis* (*M. smegmatis*), *Staphylococcus aureus* (*S. aureus*), BCG vaccine, and 6th-time reusability. Wang et al. developed an accordion-like $Ti_3C_2T_x$ MXene-based electrochemical DNA biosensor for the detection of Helicobacter pylori.[89] The developed biosensor was able to detect the complementary target DNA at less than femtomolar concentration level. In another work, W. Wei et al. proposed an MXene-based double-mode ECL-SERS immunoassay to detect *Vibrio vulnificus* (VV).[84] In the proposed biosensor, signal tags of ECL (ABEI) and specific VV antibody (Ab2) were immobilized on the surface of multifunctional MXene (R6G-$Ti_3C_2T_x$@AuNRs) as displayed in Figure 3(B). The biosensor can determine 10^2 CFU/mL VV in the SERs method and 1 CFU/ml in the ECL method. A list of the MXene-biosensors developed for the sensing of bacteria and viruses is summarized in Table 2.

3.3. Sensing cancer biomarkers

The early detection of cancer biomarkers in the human body along with utilizing the most precise and quick method is currently in demand.[90] At this point, the analytical development is possible if the biosensor is modified with a signal tag bio-recognized biomarkers such as antibodies, enzymes, deoxyribonucleic acid, ribonucleic acid, cancer cells, nucleic acid probes, or other biomolecules.[91] Herein, an interaction between sensor surface molecules and target biomarkers is usually converted to measurable electrical or optical signals. In recent advances, MXene-based 2D nonmaterial, brought a new perspective to the field of healthcare due to its higher detection sensitivity[92] in electrochemical, mass-sensitive, and optical bio-sensing.

Medetalibeyoglu et al. demonstrated an alternative, significant, good selective, and stable, SERS immunosensor for detecting carcinoembryonic antigen (CEA) in plasma samples for the early differentiation of malignant and innocent biomarkers.[93] The research group designed a 2D

Table 2. A list of MXene-based biosensors for the sensing of viruses and bacteria.

Sensing matrix	Bio-recognition element	Biosensing technique	Targeted analyte	Sensing performance			Reference
				Linear range	LOD	Detection time	
Apt_{N58}/Nb_2C-SH QDs/Au	Aptamer	SPR biosensor	SER-CoV N gene	5×10^{-2} to 100 ng m/L	4.9 pg mL^{-1}	–	[85]
ssDNA/$Ti_3C_2T_x$	DNA probe	Chemoresistive biosensor	SER-CoV-2 N gene	10^5 to 10^9 copies/mL	10^5 copies/ml	–	(W. Y. Chen et al., 2022)
dsDNA/CCB/MNP/ aptamer/$Ti_3C_2T_x$/ ZIF-8/GCE	Aptamer	ECL biosensor	HIV-1	1 fM to 1 nM	0.3 fM	–	[86]
P/T/Exo-III/Ti_3C_2 NS	DNA probe	Fluorescent sensor	HPV-18	0.5 nM to 50 nM.	100 pM	–	[87]
rpDNA/tDNA/BSA/ cpDNA/$Ti_3C_2T_x$/ Au/GCE	DNA probe	Electrochemical DNA biosensor	*Helicobacter pylori*	10^{-11} to 10^{-14} M	1.6×10^{-16} M	–	[89]
AuNPs-PNA/target DNA/Ti_3C_2 MXene	PNA probe	electrochemical sensor	*M. tuberculosis*	1×10^2 to 1×10^8 CFU m/L	20 CFU m/L	2 h	[88]
R6G-$Ti_3C_2T_x$@AuNRs-Ab2/ABEI	Antibody	Immunosensor	VV	10^2 to 10^8 CFU m/L (SERS) 1 to 10^8 CFU m/L (ECL)	10 CFU m/L 1 CFU mL^{-1}	–	[84]

MoS_2NFs@AuNPs labeled with 4-marcaptobenzoic acid as a CEASERS tag. Furthermore, the magnet-supported substrate SERS was made by Fe_3O_4@Au nanoparticles modified with delaminated $Ti_3C_2T_X$ MXene like Fe_3O_4NPs@AuNPs/d-$Ti_3C_2T_X$ MXene and was used to detect CEA. This sandwich-type immunosensor showed a linear response, high selectivity, and recovery value of 1×10^{-4}–100.0 ng m/L, 0.033 pg m/L, and around 100%, respectively. Additionally, Wu et al. claimed an efficient amino-functionalized surface plasmon resonance (SPR) N-Ti_3C_2-MXene biosensor for the sensing of CEA by signal amplification strategy.[94] In that study, the monoclonal anti-CEA capture antibody was covalently immobilized with amino silane functionalized Ti_3C_2-MXene nanosheet. Similarly, the polyclonal anti-CEA detection antibody (Ab2) was immobilized with staphylococcal protein A (SPA) decorated N-Ti_3C_2-MXene-hollow gold nanoparticles surface. The response signal was shown by the growth of Ab2-conjugated SPA/HGNPs/N-Ti_3C_2-based MXene sandwich nanostructure on the surface of SPR. This immunosensor showed a linear detection limit and range of0.15 fM and 1×10^{-3}–1×10^3 PM, respectively. M. Sharifuzzaman et al. established for the first time a low-cost detection of Apo-A1 and NMP 22 bladder cancer biomarker by a one-pot dual 2D immunosensor.[95] MXene-$Ti_3C_2T_x$ nanosheets (MXNSs) were electrodeposited at a constant potential. Next, antibodies were bonded on the MXNSs surface in the ionic medium of 4-amino-1-(4-formyl-benzyl) pyridinium bromide. MXNSs and antibody-bonded MXNSs displayed precise LOD values of 0.3 and 0.7 pg m/L, respectively. The research group observed that the micro dual integrated modified electrode yielded 7 times higher redox current than bare. Medetalibeyoglu et al. reported on the detection of prostate-specific antigen (PSA) by an immunosensor where GCE was modified by AuNPS/ATPGO along with PSA antibody 1 (Ab_1).[96] Furthermore, signal amplification PSA antibody2 (Ab_2) was labeled on delaminated MXene-gold nanoparticles (d-$Ti_3C_2T_X$MXene@AuNPs). These both modified electrodes were characterized by conventional analytical tools and other validation methods showing a linear response range and LOD of 1×10^{-2}–1.0 pg/mL and 3.0 fg/mL, respectively. Additionally, Wu et al. applied surface plasmon resonance analytical assay for point of care bio affinity assay without fluorescent or enzymatic labeling[97] to assess the presence of CEA in human serum for cancer screening and early detection. In that study, the staphylococcal protein A modified Ti_3C_2-MXene/AuNPs composites were immobilized and oriented with ferrocene of monoclonal anti-CEA antibody (Ab1) as capture. Similarly, for signal amplification, a sandwich complex was formed by introducing multiwall carbon nanotubes-PDA-silver nanoparticles-polyclonal anti-CEA antiboady2. Above all, modified electrodes have a dynamic linearity range and limit of detection of 2×10^{-16}–2×10^{-8} M and 0.07 fM, respectively.

Wang et al. presented the first real demonstration of the TNF-α cancer marker, responsible for various cancer biomarkers and inflammatory disease detection.[98] Furthermore, they concluded that the TNF-α cancer marker has a better absorption coefficient enhancing the lowest reflection and leading to phase singularity and great lateral shift (>340 μm). This plasmonic biosensor is made with a novel integration of atomic level $Ge_2Sb_2Te_2$ layer and plasmonic substrate for the capture of antibodies. Additionally, they developed a MoS_2 antibody-modified substrate used as a signal enhancer with the capability of detecting the lowest molecular level of TNF-α cancer marker and 10–15 $molL^{-1}$ limit of detection. Cheng et al. reported on lung cancer-causing, cytokeratin fragment antigen 21-1 (CYFRA21-1), which is measured as a signal tag (TB-Au-COF).[99] They have used a covalent organic framework of toluidine blue (TB) and AuNPs doped modified electrode as a substrate enhancer. The modified immunosensor has high sensitivity composites combination with Au-$Ti_3C_2T_x$ used to catch antibodies TB-Au-COF for signal unit and secondary antibodies. The detection of the CYFRA21-1 marker in the real sample displayed a dynamic linear response range and limit of detection of 0.5–1.0 $\times 10^4$ pg/mL and 0.1 pg/mL, respectively. Additionally, S. Kumar et al. chose a preferable

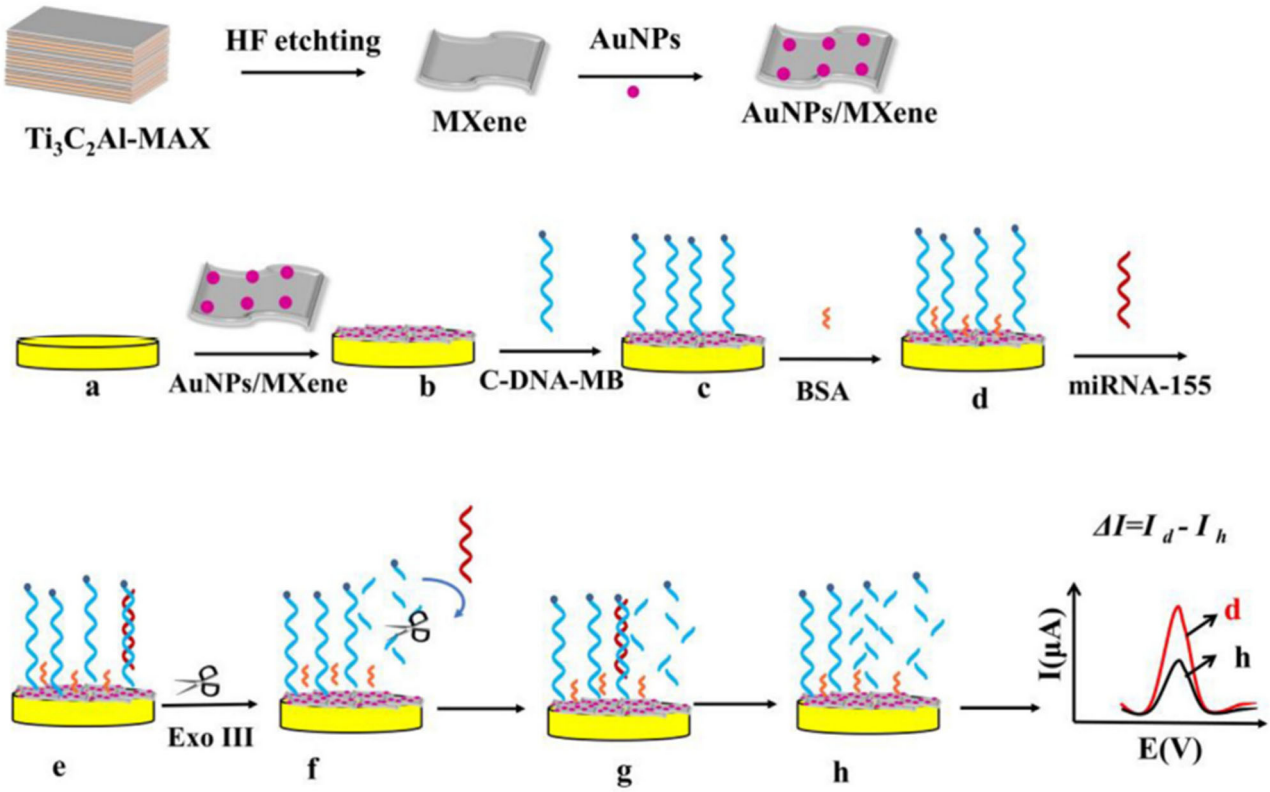

Figure 4. Schematic diagram illustrating the miRNA-155 biosensor fabricated on AuNPs modified Ti_3C_2 (MXene) nanocomposite designed with Exo III-leveled cascade target method. Individuals are (a) Au-Electrode, (b) AuNPs functionalizedTi_3C_2 (MXene) modified Au-Electrode, (c) C-DNA immobilized AuNPs functionalized Ti_3C_2 (MXene) modified Au-Electrode, (d) BSA/C-DNA immobilized AuNPs functionalized Ti_3C_2 (Mxene) modified Au-Electrode, (e) miRNA-155/BSA/C-DNA immobilized AuNPs functionalized Ti_3C_2 (MXene) modified AuE, (f–h) Exo III/miRNA-155/BSA/C-DNA immobilized AuNPs functionalized Ti_3C_2 (MXene) modified Au-Electrode.

detection of CEA in which hexaammineruthenium ($[Ru(NH_3)_6]^{3+}$) redox probe was prepared by minimally intensive layer delaminated Ti_3C_2-MXene nanosheet with amino silane (with APTES) immobilizing bio-receptor (anti-CEA).[32] This biofunctionalized immunosensor has 1×10^{-4}–2000 ngm/L linear dynamic range and 37.9 $\mu Ang^{-1} mLcm^{-2}$ sensitivity per decade showing a better performance than previously reported 2D nanomaterials modified electrode. Zhang et al. proposed CuAu-layered double hydroxide (LDH) multifunctional Ti_3C_2-MXene-based immunosensors with excellent conductivity rendering electron movement between interchangeable anions for the detection of CEA.[100] The proposed immunosensor displayed a wide detection range of 1×10^{-4}–80 ng/mL and the lowest current of detection at 33.6 fg/mL(SWV), and 45.4 $fg.mL^{-1}$ (i-t), reflecting excellent analytical capability. Tian et al., prepared ferrocene(Fc)-modified HDNA2 N-carboxymethyl chitosan/Mo_2C biosensors to capture hairpin DNA1 and hairpin DNA2 in the presence of miRNA-21.[101] By monitoring the Fc redox signal, miRNA-21 was detected as a strand displacement reaction. The fabricated chitosan/Mo_2C multifunctional amine groups nanocomposite has a strong affinity to the DNA probe with a linear range of 1.0 FM–1.0 nM, and LOD of 0.34 fM. In addition, Wang et al. demonstrated an aptasensor for the detection of breast cancer biomarker, Mucin1 in [102]. The MXene(Ti_3C_2) surface was fabricated with complementary DNA and Fc (cDNA-Fc/MXene) and later Micin1 was bound with Au-S linkage. In this detection mechanism, the decrease of the electrical signal between the detach rate of cDNA-ferrocene/MXene probe-Mucin1 complex and the corresponding binding signal was measured. The developed sensor offered a dynamic linear range of 1.0 pM–10 μM and a LOD of 0.33 pM, thus suitable for clinical diagnosis applications. Moreover, Yang et al. reported on the immobilization of captured DNA by forming Au-S bonding on the surface of AuNPs/Ti_3C_2 MXene nanocomposite and methylene blue (MB) modification on the 3 ends of the C-DNA.[91] A double-stranded structure was formed in the presence of miRNA-155 and C-DNA. Next, during the reaction, ds-DNA was formed between miRNA-155 and C-DNA by base pairing. Furthermore, several C-DNA was released at different experimental conditions increasing the peak current differences. Overall, the developed biosensor showed desirable stability, reproducibility, specificity, LOD of 0.35 fM, and linear response range of 1.0 fM–10 nM. Figure 4 shows a schematic illustration of the developed biosensor.

Similarly, duplex-specific nuclease (DSN)-based AuNPs/MXene—for reliable detective signal amplification biosensor was introduced by Mohammadniaei et al., where multiple microRNAs were detected by the one-step process in the real sample for RNA-21 and microRNA-141.[] A large number of DNA probes were immobilized on dual screen-printed electrode of ($Ti_3C_2T_x$-AuNPs) by bonding with S-Au. This method reduced the detection (assay) time to 80 minutes for signal amplification to render the

Table 3. List of reported MXene-modified biosensors along with their performance.

Electrode	Target biomarker	Sensing performance		Reference
		LOD	Linear range	
Anti-CEA/Fe_3O_4 NPs@Au NPs/d-$Ti_3C_2T_X$	CEA	0.033 pg mL^{-1}	0.0001–100.0 ng mL^{-1}	[93]
N-Ti_3C_2-MXene/HGNPs/SPA/Ab2	CEA	0.15 fM.	0.001–1000 pM	[94]
MXNSs-AFBPB-film-modified DIDμE	Apo-A1 and NMP 22	0.3 and 0.7 pg mL^{-1}	0.1 pg mL^{-1} to 50 ng mL^{-1})	[95]
d-$Ti_3C_2T_X$ MXene@AuNPs/Ab2	PSA	3.0 fg mL^{-1}	0.01–1.0 pg mL^{-1}	[96]
Ti_3C_2-MXene/AuNPs/SPA	CEA	0.07 fM	2×10^{-16}–2×10^{-8} M	[97]
$Ge_2Sb_2Te_5$ with plasmonic substrate	TNF-α	10–15 M	10 fM–10 μM	[98]
GCE/Au-$Ti_3C_2T_x$/Ab1/BSA/CYFRA21-1/Ab2-TB-Au-COF	CYFRA21-1	0.1 pg·mL^{-1}	0.5–1.0 $\times 10^4$ pg·mL^{-1}	[99]
Anti-CEA/f-Ti_3C_2-MXene/GC	CEA	37.9 μAng^{-1}mLcm^{-2}	0.0001–2000 ngmL^{-1}	[32]
Ti_3C_2@CuAu-LDH-Ab2	CEA	33.6 fg/mL and 45.4 fg/mL	0.0001–80 ng/mL	[105]
GCE/NCS/Mo_2C nanosheet/p-DNA/HDNA1&HDNA2-Fc	microRNA-21	0.34 fM	1 fM–1 nM	[101]
cDNA-Fc/MXene/Apt/Au/GCE	MUC1	0.33 $\times 10^{-3}$nM	0.001–1.0 $\times 10^4$ nM	[102]
Exo III/miRNA-155/BSA/C-DNA/AuNPs/Ti_3C_2 MXene/AuE	microRNA-155	0.35 fM	1.0 f.M–10 nM	[91]
AuNP@MXene/Au-ssDNA	miR-21 and miR-141	204 aM and 138 aM	500 aM–50 nM	
SOx/MXene-Chi/GCE	sarcosine	18 nM	7.8 μM–18 nM	[103]
FAD/$Ti_3C_2T_x$/GCE	H_2O_2	0.7 nM	5 nM–2 μM	[104]

physicochemical properties. The developed 96-well biosensor device displayed an outstanding sensitivity at 204 and 138 aM of detection limit showing excellent biosensing capacity. Additionally, Hroncekova et al., fabricated a highly sensitive sarcosine oxidase enzyme-modified electrode on 2D $Ti_3C_2T_x$ MXene/chitosan nanocomposite, detecting sarcosine, a prostate cancer biomarker, was detected in a real urine sample.[103] This protein-modified biosensor has excellent operational parameters supported with chitosan and characterized by atomic force and scanning electron microscopies. The developed protein biosensor had a response time of 2 seconds, recovery indexing of 102.6%, detection limit of 18 nM, and a linear response up to 7.8 µM.

Furthermore, Nagarajan et al. reported a successful modification of the flavin adenine dinucleotide (FAD)-$Ti_3C_2T_x$ adhesion immobilized electrode to overcome poor electron transfer properties.[104] They found the modified FAD electrode to be dependent on pH level, stable at −0.455 V, and showed an electro-catalytic H_2O_2 reduction at −0.47 V. Here, the developed electrochemical biosensor showed a linear response range of 5 nM–2 µM when detecting H_2O_2 in ovarian cancer cells, detection found linearity. In the presence of interfering molecules, the selectivity of the modified electrode was comparatively as high as 0.125 µA nM/cm^2. A list of the reported MXene-modified biosensors along with their performance parameters such as detection limit, linear response range, and the target biomarkers are summarized in Table 3.

3.4. Sensing food contaminates/mycotoxins

As the global population continues to increase, the demand for food safety also increases. Screening the quality of agro-products is an effective strategy for assuring global food safety.[106] Several contaminants are found in agro-products including mycotoxins, gliotoxin, endotoxin, microorganisms, exosomes, pesticides, antibiotics, and heavy metals. Among those, mycotoxins and gliotoxins are the most poisonous and chemically stable compounds which are found in various genera of filamentous fungi.[100] Typically, mycotoxins can grow on a variety of crops and food-related items such as grains, nuts, maize apples, dried fruits, cereals, and spices under warm, damp, and humid conditions. Several health effects such as cancer and immune deficiency are caused by mycotoxin and thus threatened humans, animals, and livestock.[107,108] Recently, various types of mycotoxins were identified including patulin (PAT), citrinin (CIT), aflatoxin (AF), zearalenone (ZEN), and ochratoxin (OTA), T-2 toxin, and fumonisins-B_1/B_3 (FB_1-FB_3). Generally, it can be exposed directly or indirectly and cannot be easily removed from food items.[109] Similarly, gliotoxin is a type of mycotoxin that contains sulfur, belongs to a group of naturally produced peptides (piperazine-2,5-dione), and is considered one the most toxic metabolite produced by few species of fungi such as *Aspergillus fumigatus* causing severe problems to the environment.[110]

A reliable and sensitive identification strategy is required to ensure food safety against mycotoxins/gliotoxins. Various conventional methods were used to identify the food contaminants such as thin-layer chromatography, gas chromatography, high-performance liquid chromatography, mass spectrometer, and gas and liquid chromatography-mass spectrometers.[111] However, some drawbacks were formulated by using these conventional methods including requiring a variety of assay steps, demanding skill manpower, and calling for tedious pretreatment. Therefore, it is urgently required to introduce a prompt, novel, convenient, sensitive, reliable, and stable detection technique to ensure the effective detection of mycotoxin contaminants.[112] Meanwhile, biosensors with MXene-based nanomaterials were significantly explored for the detection of food contaminants during the last decade. Owing to its outstanding physicochemical properties, MXene is considered one of the superior materials that are widely used in the development of biosensors.[26] Researchers focused recently on the development of MXene-based biosensors for food contaminants screening applications. A schematic diagram illustrating the structure of MXene nanomaterials-based biosensor for sensing food contaminants in agro-products is demonstrated in Figure 5.[100]

Aflatoxin (AF) is a well-known and most toxic, mutagenicity, carcinogenic, and teratogenicity mycotoxin present in many natural agricultural foods, and includes AFB_1, AFB_2, AFG_1, AFG_2, AFM_1, and AFM_2.[113] The maximum content

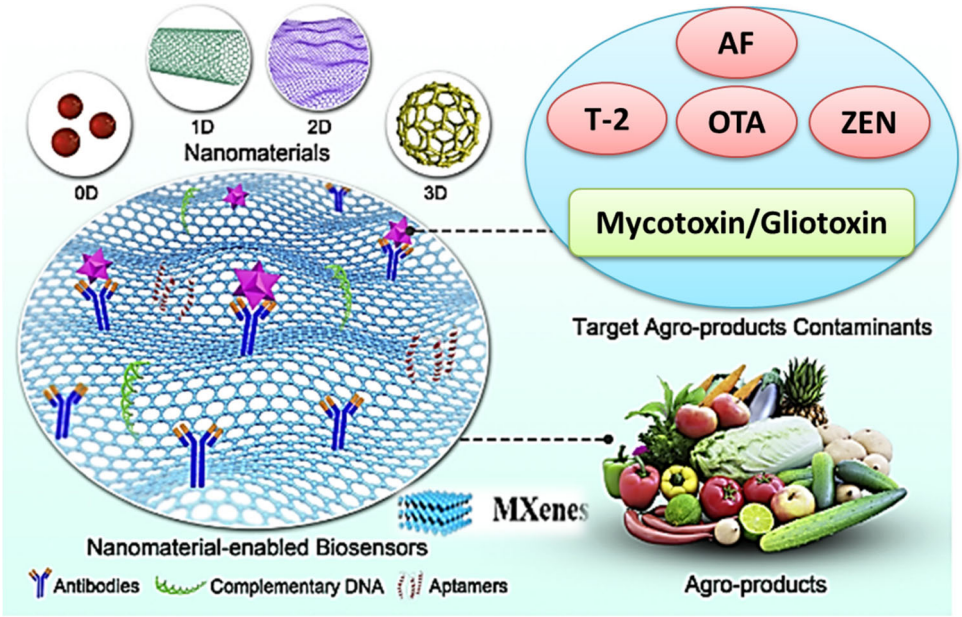

Figure 5. Schematic diagram of MXene-based nanomaterial biosensor for the detection of food contaminants.[100]

of AFB_1 in cereal foods is 2.00 ppb from the total content of AF (4.0 ppb) and is thus considered as most toxic.[114] Wu et al. developed a ratiometric SERS aptasensor for detecting AFB_1 in agricultural food. The loaded AFB_1 aptamer was modified using AuNPs followed by 4,4′-Vinylenedipyridine as the trigger is shown in Figure 6(A). The extensive SERS hot spots and the MXene nanosheets were formed by the chelation and hydrogen bonding between the aptamer and MXene. The experimental results revealed a linear concentration range of 1×10^{-3}–100 ng m/L and LOD of 0.6 pg m/L suggesting the proposed sensor (AuNPs/Mxene SERS substrate) has a great potential for the detection of AFB_1 in food contents.[113] Ochratoxin (OTA) is another type of mycotoxin present in agro-products and can cause hepatopathy in both humans and animals. The maximum content of OTA in cereal foods is 5.00 ppb, and thus it is very difficult to detect OTA from agricultural products.[116] Zheng et al. developed a ratiometric SERS aptasensor for the reproducible and sensitive detection of OTA.[115] The synthesized Au-Ag NPs showed strong amplification and stable SERS activity with the assistance of 2-mercaptobenzoimidazole-5-carboxylic acid (MBIA). The stable and unique MXene nanosheets were fabricated with Au-Ag NPs and that mostly depended on the reaction between hydrogen bond and the chelation of OTA aptamer as shown in Figure 6(B). In optimal conditions, the proposed immunosensor indicated a linear response in a concentration range of 0.01–50 nM with LOD of 1.28 pM to detect AFB1. Additionally, the developed biosensor was applied to red wine samples with good recovery range of 93.31–97.44% with a relative standard deviation of 2.65% to detect OTA. A secondary metabolite mycotoxin causing acute and chronic toxicity and found in a variety of soil fungi are known as T-2 toxin.[100] Lately, researchers had a greater interest to detect T-2 toxins using various nanomaterials such as carbon nanotubes (CNTs), gold nanoparticles (AuNPs), and up conversion nanoparticles (UCNPs), multi-wall carbon nanotube (MWCNT), magnetic nanoparticles (MNPs), and single-wall carbon nanotube (SWCNT). The development of AuNPs and SWCNTs-based immunosensor was studied for the detection of T-2 toxin. The complementary DNA (cDNA) and the T-2 aptamer were combined with MNPs, and UCNPs, respectively, and formed a hybrid aptamer conjugate.[117] A 3D stem-loop structure was fabricated through a bounding T-2 aptamer. They observed that the electrochemical signal reduced with decreasing the number of T-2 antibodies and anti-mouse secondary antibodies, respectively. The experimental results revealed a good linear response in the concentration range of 0.1–100 ng mL^{-1} for sensing T-2 toxin. Additionally, the developed detector was applied in real food samples and found a good recovery range of 95.97–104.00% which indicates the great potential of the proposed sensor for detecting T-2 toxin in food contents. The well-known vomitoxin, known as deoxynivalenol (DON), is found in *Fusarium graminearum and F. culmorum*. MXene sheets synthesized by selective etching of aluminum (Al) was incorporated into an immobilized tailor-made DON aptamer biosensor as presented in Figure 6(C).[36] FESEM and XPS indicated the etching on the MXene layers and further the composition of Ti-Fx and TiO_2 as a result of the substitution of Al into O and F endings. The developed sensor showed a linear relationship (1 fg m/L–1 ng m/L) and the limit of detection of 1.0 fg m/L. The developed DON aptasensor displayed an outstanding selectivity against deoxynivalenol when compared with other mycotoxins such as zearalenone and ochratoxin. The proposed sensitive sensor proved to effective biosensor to detect DON in food and feed samples.

Additionally, gliotoxin is another toxic metabolite found in a few species of fungi such as the growth of *aspergillus fumigatus* causes serious problems to human health and animals. Recently, MXene-based electrochemical biosensor for sensing gliotoxin attracted the attention of several research groups. Wang et al. reported on the modified MXene nanosheets-based DNA electrochemical biosensor to detect

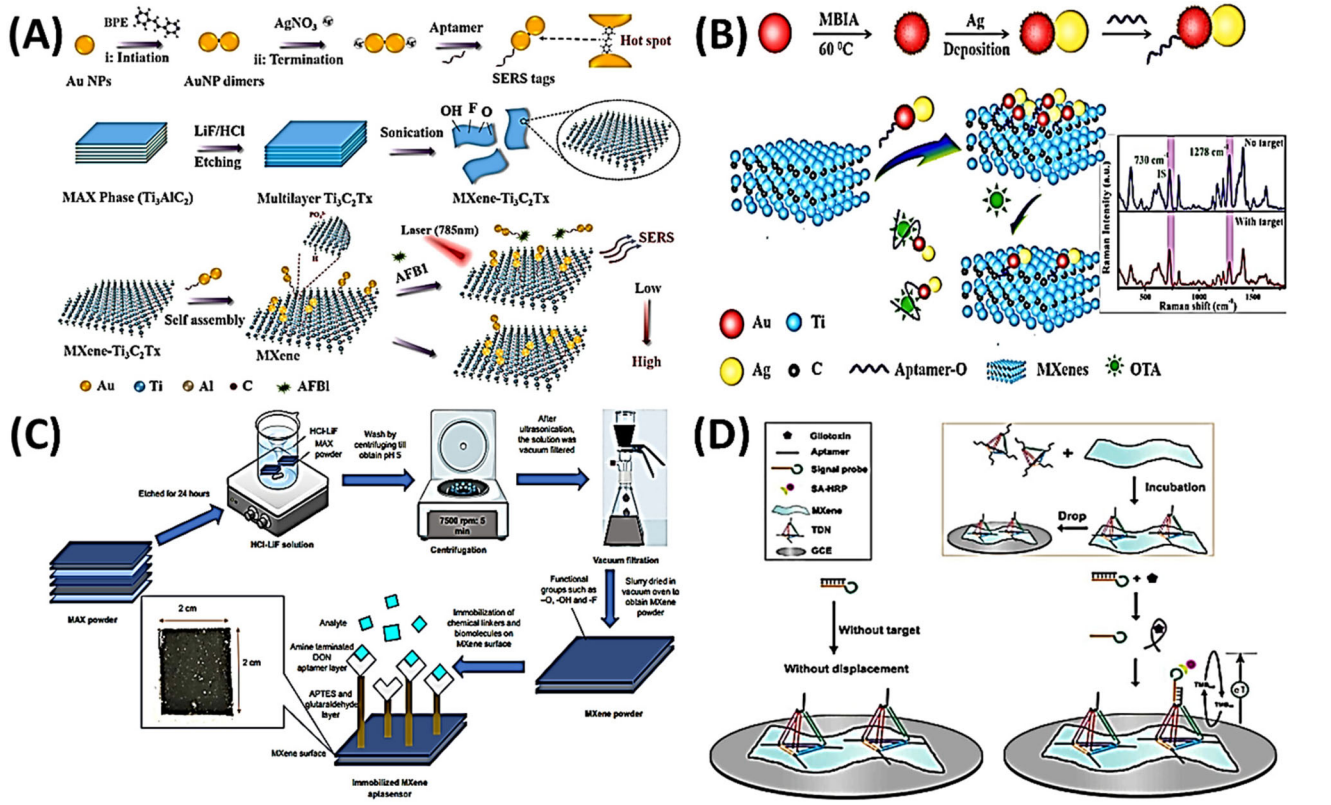

Figure 6. Schematic diagram of (A) AuNP dimers/MXene-based surface-enhanced Raman spectroscopy aptasensor for the identification of AFB_1,[113] (B) Au-Ag Janus NPs modified MXene-based aptasensor for the identification of ochratoxin,[115] (C) Ti_3C_2-MXene immobilized aptasensor for the detection of DON,[36] and (D) TDN/MXene based modified biosensor for the identification of gliotoxin.[110]

gliotoxin.[110] Firstly, the MXene nanosheet surface was immobilized with tetrahedral DNA (TDNs) nanostructures through the chemical reaction of the phosphate group of DNA and the titanium. The modified DNA probes exhibited good conductivity that enhanced the electron transfer between the electrode surface and the electrochemical species. Therefore, a unique and efficient TDN-based electrode containing target molecules were fabricated generating strong electrochemical signals as shown in Figure 6(D). It was observed in optimal conditions that the developed electrochemical sensor demonstrated a wide linear range of 5 pM–10 nM with a limit of detection of 5 pM. Furthermore, the sensitive Mxene-based electrochemical biosensor was tested in human serum samples with a good recovery (96.3–115%) recording a new detection system for sensing other mycotoxins.

3.5. Sensing hazardous environmental pollutants

Around our surrounding environment, there are so many hazardous materials. The U.S. Environmental Protection Agency (EPA) reported 187 pollutants emitted from vehicles, various industrial sectors, and other mobile sources.[] The long-term effects and chronic diseases associated with this environmental pollution cause worldwide public health problems. This poisoning has several adverse health impacts such as cancer, including lung, kidney, bone, and stomach; harm to the nervous system and brain; birth defects; irritation to the eyes, nose, and throat; coughing and wheezing; impaired lung function; harm to the cardiovascular system; and reduced fertility.[118–123]

Hazardous environmental pollutants are a major drawback of modern civilization, and thus there are global urgent demands for their detection, reduction, and gradual elimination. There are many reported methods for the detection of hazardous environmental pollutants including atomic adsorption spectrometry,[124] and inductively-coupled plasma mass spectrometry,[125] inductively-coupled plasma atomic emission spectrometry.[126] Furthermore, recent techniques are using colorimetric, fluorometric or electrochemical methods.[127–129] Additionally, electrochemiluminescence and photoelectrochemical detectors were used as evolutionary electro-analysis techniques offering substantial progress.[27]

These conventional sensing techniques demand huge instrumentations and are not appropriate for in-situ and online identification. Alternately, quartz-enhanced laser photoacoustic spectroscopic (QE-LPAS) technology emerged recently as one of the most powerful techniques for the detection of hazardous materials in environmental and medical sciences,[130] however, they are expensive method. As earlier discussed, there are extraordinary developments in nanotechnology and nano-science, and numerous nanomaterials were reported for electrochemical sensing applications. Furthermore, MXene nanostructures have lately attracted plenty of interest in the identification of hazardous materials.[131,132] Different detection methods incorporating MXene compounds for the detection of hazardous materials

Table 4. Detection performance of MXene-biosensors for hazardous materials.

MXene-biosensor	Analytes	Methods	Sensing performance			References
			LOD	Linearity range	Reproductivity	
Hb in Chit-[bmim]PF_6-TiO_2-Gr/GCE	H_2O_2	Amperometric	0.3 μM	1–1170 (μM)	95%/20 days	[133]
Nafion/Hb/MXene-Ti_3C_2/GCE	$NaNO_2$	Cyclic voltammograms (CVs)	0.12 μM	0.5–11,800 (μM)	Stable & reproducible	[134]
AChE/CS-$Ti_3C_2T_x$/GCE	Organophosphorous pesticides (OPs)	Cyclic voltammetry (CV)	0.3×10^{-14} M	1×10^{-14}–1×10^{-8} M	85.39%/20 days	[135]
AChE-Chit/Ti_3C_2/Au NPs/MnO_2/Mn_3O_4/GCE	Methamidophos	Differential pulse voltammetry (DPV)	1.34×10^{-13} M	10^{-12}–10^{-6} M	80.7%/21 days	[136]
$Ti_3C_2T_x$/Au-Pd/GA/AChE	Paraoxon	Amperometric	1.75 ng.m L^{-1}	0.1 – 1000 μg.mL^{-1}	95%/7 days	[137]

were reported such as electrochemical biosensors, electrochemical non-biosensors, electrochemiluminescence sensors, photoelectrochemical sensors, and flexible sensors.[27] Here, we focus mainly on MXene-based biosensors used for the detection of hazardous materials.

A pioneer work (not MXene-based biosensor) describing an enzyme-based biosensor developed by Lia et al. for the detection of hydrogen peroxide, a hazardous material, via easy and effective enzyme immobilization (Lia et al., 1996). They reported on the immobilization of horseradish peroxidase in a silica sol-gel matrix on a carbon paste electrode. By using an amperometric method, the operating potential of the working electrode, mediator concentration and pH level, and thermal stability, led to an optimal analytical performance along with a linear calibration for H_2O_2 in the range of 2.0×10^{-5}–2.6×10^{-3} M.

A desirable electrochemical response of the reduction of H_2O_2 in the range of 1–1170 μM was demonstrated by a TiO_2-G nanocomposite-based biosensor, synthesized by hydrolysis of titanium tetraisopropoxide (TTIP) in a colloidal suspension of GO and in-situ hydrothermal treatment.[133] At room temperature, the direct electrochemistry and electrocatalysis of hemoglobin ionic liquid, 1-Butyl-3-methylimidazolium hexafluorophosphate, chitosan, and TiO_2-graphene nanocomposite modified GCE was examined in this report.

Liu et al. first reported on the detection of $NaNO_2$ utilizing MXene-Ti_3C_2 composite in a mediator-free biosensor.[134] A. In this report, MXene-Ti_3C_2 facilitated the direct electron transfer of Hb, and the biosensor displayed a wide linear range of 0.5–11,800 μM for sensing $NaNO_2$ with a low detection limit of 0.12 μM. Thus, it is evident that the developed sensor can be a promising choice for effective enzyme immobilization in environmental analysis.

Exposure to organophosphorus (OP) pesticides (highly toxic) is considered hazardous as it sometimes causes health issues. Acetylhydrolase biosensors based on transition metal carbides (MXenes) nanosheets and chitosan were developed and reported[135] for the detection of OPs. The electrochemical behavior of the AChE/CS-$Ti_3C_2T_x$/GCE biosensor was investigated by CV and EIS showing a detection limit of 0.3×10^{-14} M. Owing to the outstanding biocompatibility, no-toxicity, film-forming ability, the developed biosensor showed acceptable reproducibility, satisfactory stability, and anti-interference ability. As environmental contaminants are routinely released into the atmosphere forming organophosphate pesticides (OPs) that find their way to agricultural activities. Song et al. designed a promising biosensor, AChE-Chit/Ti_3C_2/Au NPs/MnO_2/Mn_3O_4/GCE for the detection of Ops.[136] Under the optimal conditions, the designed biosensor had a very low limit of detection of 1.34×10^{-13} M, and further, the feasibility of the developed biosensor for sensing methamidophos in real samples was proven with outstanding recoveries (95.2%–101.3%). Most recently, a similar report was published on the detection of toxic elements, Paraoxon, with a great low limit of detection.[137] A summary of MXene-biosensors along with performance is presented in Table 4.

4. Advantages and shortcoming of MXene based biosensor

The popularity of MXene in biosensing application has arisen from its excellent bio-compatibility and electro-optical properties. Owing to good biocompatibility and abundant anchoring sites, MXene based biosensor's transducer can be loaded proteins, enzymes, nucleic acids easily which is the main advantage of MXene-based biosensor for sensing prospects. The excellent electro-optical properties of MXene become helpful for translating the bio-signals into desired optical or electrical signal. Those properties are very important to developed for fabrication of ultrasensitive, stable biosensor for detection of bio-analytes. However, the shortcoming of MXene based biosensor includes damages of analytes during analysis, time consuming methods of MXene synthesis, complex to characterize MXene on the transducer surface. The characterizing techniques Scanning electron microscope (SEM), X-ray photoelectron spectroscopy (XPS), nuclear magnetic resonance spectroscopy (NMR), neutron scattering, X-ray atomic pair distribution function (X-ray PDF), scanning transmission electron microscopy (STEM) are used to characterized MXene on the transducer surface but they still understood the surface termination poorly.

5. Future perspective of MXene-based biosensor as a next-generation diagnostics tool

Recent studies on the fabrication of biosensing platforms by using MXene-based nanocomposite revealed that MXene is one of the best candidates among nanomaterials for upgrading biosensing technology. MXene is a promising 2D material for the development of wearable biosensors as the next-generation diagnostics tool. Designing new MXene based skin inspired sensors other than titanium carbide with large tunable strain, high sensitivity, high stretchability and low device dimension to be easily integrated into wearable nanoelectronics is highly challenging. Advancements in wearable strain sensors will lead to detect ultra-weak pressure such as artery pulses or other low strain physical stimuli. Mechanism optimization of such wearable strain sensors will be highly beneficial for studying human motion, robotic systems and prosthetic devices. So, MXene-based wearable biosensors are still in the early phases of development, and more improvement is necessary for potential realization for actual routine applications. The major challenges to be solved for developing MXene-based wearable biosensing technology are the low stability of MXene in an oxygenated solvent, the difficulties in producing MXene on large scale, and the surface defects and cytotoxicity of MXene. So, it is critical to solve technological difficulties for commercializing MXene-based wearable biosensors as a next-generation diagnostic tool. The next generation of diagnostic tools should focus on (1) expanding sensing devices to a wide panel for tracking human health conditions at the molecular level, (2) monitoring biomolecules at very low concentrations, and (3) producing safe and reliable diagnostic platforms. By obtaining improvements in fabrication techniques, surface functionalization, and integration capabilities, this sector is projected to further improve. In the future, the continuation in advancing the research for innovative nanostructures, surface modification strategies, or synthesis methodology will serve as the foundation for commercializing MXene nanocomposites in the development of enhanced wearable electrochemical biosensing technologies.

6. Conclusion

Developing ultra-sensitive and ultra-selective biosensors is one of the most prominent challenges facing the advancement of sensors for biomedical applications. During the last decade, various 2D materials were proposed to develop biosensors with superior sensitivity and selectivity. Owing to its overwhelming phenomenal properties and the plethora of tailorable surface function groups, MXene is among the best 2D materials for the development of biosensors with high performance and excellent sensitivity, and outstanding selectivity. Here, we shed light on the structure, synthesis techniques, and functionalization methods of MXenes. Additionally, MXene-based detection platforms in different sensing applications are survived. An emphasis had been made on reviewing the applications of MXenes in the detection of biomolecules, pathogenic bacteria and viruses, cancer biomarkers food contaminants and mycotoxins, and hazardous pollutants. Lastly, the potential of using MXene-based biosensors as a next-generation diagnostics tool is discussed. Furthermore, the potential of MXenes for developing innovative detection mechanisms is explored by providing visionary approaches for materials science and sensing communities.

Disclosure statement

The authors declared that they have no known competing financial interests

References

[1] Ma, X.; Youngblood, N.; Liu, X.; Cheng, Y.; Cunha, P.; Kudtarkar, K.; Wang, X.; Lan, S. Engineering Photonic Environments for Two-Dimensional Materials. Nanophotonics **2021**, *10*, 1031–1058. DOI: 10.1515/nanoph-2020-0524.

[2] Pacilé, D.; Meyer, J. C.; Girit, Ç. Ö.; Zettl, A. The Two-Dimensional Phase of Boron Nitride: Few-Atomic-Layer Sheets and Suspended Membranes the Two-Dimensional Phase of Boron Nitride: Few-Atomic-Layer Sheets. *Appl. Phys. Lett.* **2008**, *92*, 133107. DOI: 10.1063/1.2903702.

[3] Seo, J. W.; Jun, Y. W.; Park, S. W.; Nah, H.; Moon, T.; Park, B.; Kim, J. G.; Kim, Y. J.; Cheon, J. Two-Dimensional Nanosheet Crystals. *Angew. Chem. Int. Ed. Engl.* **2007**, *46*, 8828–8831. 10.1002/anie.200703175.

[4] Takahashi, N.; Hata, H.; Kuroda, K. Exfoliation of Layered Silicates through Immobilization of Imidazolium Groups. *Chem. Mater.* **2011**, *23*, 266–273. DOI: 10.1021/cm102942s.

[5] Feng, A.; Yu, Y.; Wang, Y.; Jiang, F.; Yu, Y.; Mi, L.; Song, L. Two-Dimensional MXene Ti_3C_2 Produced by Exfoliation of Ti_3AlC_2. *Mater. Des.* **2017**, *114*, 161–166. DOI: 10.1016/j.matdes.2016.10.053.

[6] Gonzalez-Julian, J. Processing of MAX Phases: From Synthesis to Applications. *J. Am. Ceram. Soc.* **2021**, *104*, 659–690. DOI: 10.1111/jace.17544.

[7] Barsoum, M.; El-Raghy, T. The MAX Phases: Unique New Carbide and Nitride Materials. *Am. Sci.* **2001**, *89*, 334. DOI: 10.1511/2001.4.334.

[8] Chen, W. Y.; Lin, H.; Barui, A. K.; Gomez, A. M. U.; Wendt, M. K.; Stanciu, L. A. DNA-Functionalized Ti3C2T xMXenes for Selective and Rapid Detection of SARS-CoV-2 Nucleocapsid Gene. *ACS Appl. Nano Mater.* **2022**, *5*, 1902–1910. DOI: 10.1021/acsanm.1c03520.

[9] Barsoum, M. W. The MN + 1AXN Phases: A New Class of Solids. *Prog. Solid State Chem.* **2000**, *28*, 201–281. DOI: 10.1016/S0079-6786(00)00006-6.

[10] Mashtalir, O.; Naguib, M.; Mochalin, V. N.; Dall'Agnese, Y.; Heon, M.; Barsoum, M. W.; Gogotsi, Y. Intercalation and Delamination of Layered Carbides and Carbonitrides. *Nat. Commun.* **2013**, *4*, 1–7. DOI: 10.1038/ncomms2664.

[11] Zamhuri, A.; Lim, G. P.; Ma, N. L.; Tee, K. S.; Soon, C. F. MXene in the Lens of Biomedical Engineering: Synthesis, Applications and Future Outlook. *Biomed. Eng. Online.* **2021**, *20*, 1–24. DOI: 10.1186/s12938-021-00873-9.

[12] Naguib, M.; Mashtalir, O.; Carle, J.; Presser, V.; Lu, J.; Hultman, L.; Gogotsi, Y.; Barsoum, M. W. Two-Dimensional Transition Metal Carbides. *ACS Nano.* **2012**, *6*, 1322–1331. 10.1021/nn204153h.

[13] Li, Z.; Zhuang, Z.; Lv, F.; Zhu, H.; Zhou, L.; Luo, M.; Zhu, J.; Lang, Z.; Feng, S.; Chen, W.; et al. The Marriage of the FeN_4 Moiety and MXene Boosts Oxygen Reduction Catalysis: Fe 3d Electron Delocalization Matters. *Adv. Mater.* **2018**, *30*, 1803220–1803228. DOI: 10.1002/adma.201803220.

[14] Boota, M.; Anasori, B.; Voigt, C.; Zhao, M. Q.; Barsoum, M. W.; Gogotsi, Y. Pseudocapacitive Electrodes Produced by

Oxidant-Free Polymerization of Pyrrole between the Layers of 2D Titanium Carbide (MXene). *Adv. Mater.* **2016**, *28*, 1517–1522. 10.1002/adma.201504705.

[15] Sun, R.; Zhang, H.; Bin; Liu, J.; Xie, X.; Yang, R.; Li, Y.; Hong, S.; Yu, Z. Z. Highly Conductive Transition Metal Carbide/Carbonitride(MXene)@Polystyrene Nanocomposites Fabricated by Electrostatic Assembly for Highly Efficient Electromagnetic Interference Shielding. *Adv. Funct. Mater.* **2017**, *27*, 1702807–1702811. DOI: 10.1002/adfm.201702807.

[16] Gao, Z. W.; Zheng, W.; Lee, L. Y. S. Highly Enhanced Pseudocapacitive Performance of Vanadium-Doped MXenes in Neutral Electrolytes. *Small.* **2019**, *15*, 1902649. DOI: 10.1002/smll.201902649.

[17] Bao, W.; Shuck, C. E.; Zhang, W.; Guo, X.; Gogotsi, Y.; Wang, G. Boosting Performance of Na-S Batteries Using Sulfur-Doped $Ti_3C_2T_x$ MXene Nanosheets with a Strong Affinity to Sodium Polysulfides. *ACS Nano.* **2019**, *13*, 11500–11509. 10.1021/acsnano.9b04977.

[18] Huang, W.; Hu, L.; Tang, Y.; Xie, Z.; Zhang, H. Recent Advances in Functional 2D MXene-Based Nanostructures for Next-Generation Devices. *Adv. Funct. Mater.* **2020**, *30*, 2005223–2005232. DOI: 10.1002/adfm.202005223.

[19] Karahan, H. E.; Goh, K.; Zhang, C.; Yang, E.; Yıldırım, C.; Chuah, C. Y.; Ahunbay, M. G.; Lee, J.; Tantekin-Ersolmaz, B.; Chen, Y.; Bae, T. H. MXene Materials for Designing Advanced Separation Membranes. *Adv. Mater.* **2020**, *32*, 1906697. DOI: 10.1002/adma.201906697.

[20] Hui, X.; Ge, X.; Zhao, R.; Li, Z.; Yin, L. Interface Chemistry on MXene-Based Materials for Enhanced Energy Storage and Conversion Performance. *Adv. Funct. Mater.* **2020**, *30*, 2005190. DOI: 10.1002/adfm.202005190.

[21] Chia, H. L.; Mayorga-Martinez, C. C.; Antonatos, N.; Sofer, Z.; Gonzalez-Julian, J. J.; Webster, R. D.; Pumera, M. MXene Titanium Carbide-Based Biosensor: Strong Dependence of Exfoliation Method on Performance. *Anal. Chem.* **2020**, *92*, 2452–2459. 10.1021/acs.analchem.9b03634.

[22] George, S. M.; Kandasubramanian, B. Advancements in MXene-Polymer Composites for Various Biomedical Applications. *Ceram. Int.* **2020**, *46*, 8522–8535. DOI: 10.1016/j.ceramint.2019.12.257.

[23] Sinha, A.; Zhao, H.; Huang, Y.; Lu, X.; Chen, J.; Jain, R. MXene: An Emerging Material for Sensing and Biosensing. *TrAC - Trends Anal. Chem.* **2018**, *105*, 424–435. DOI: 10.1016/j.trac.2018.05.021.

[24] Riazi, H.; Taghizadeh, G.; Soroush, M. MXene-Based Nanocomposite Sensors. *ACS Omega.* **2021**, *6*, 11103–11112. 10.1021/acsomega.0c05828.

[25] Sinha, A.; Dhanjai; Mugo, S. M.; Chen, J.; Lokesh, K. S. MXene-Based Sensors and Biosensors: Next-Generation Detection Platforms. In *Handbook of Nanomaterials in Analytical Chemistry: Modern Trends in Analysis*; Elsevier Inc., **2019**. DOI: 10.1016/B978-0-12-816699-4.00014-1.

[26] Yoon, J.; Shin, M.; Lim, J.; Lee, J.-Y.; Choi, J.-W. Recent Advances in MXene Nanocomposite-Based Biosensors. *Biosensors.* **2020**, *10*, 185. DOI: 10.3390/bios10110185.

[27] Wu, X.; Ma, P.; Sun, Y.; Du, F.; Song, D.; Xu, G. Application of MXene in Electrochemical Sensors: A Review. *Electroanalysis.* **2021**, *33*, 1827–1851. DOI: 10.1002/elan.202100192.

[28] Yuan, X.; Zhang, M.; Wu, Y. MXene-Based Sensors for Detecting Human Physiological Information. *Sens. Mater.* **2020**, *32*, 4047–4065. DOI: 10.18494/SAM.2020.2990.

[29] Rasool, K.; Helal, M.; Ali, A.; Ren, C. E.; Gogotsi, Y.; Mahmoud, K. A. Antibacterial Activity of $Ti_3C_2T_x$ MXene. *ACS Nano.* **2016**, *10*, 3674–3684. 10.1021/acsnano.6b00181.

[30] Dwivedi, N.; Dhand, C.; Kumar, P.; Srivastava, A. K. Emergent 2D Materials for Combating Infectious Diseases: The Potential of MXenes and MXene-Graphene Composites to Fight against Pandemics. *Mater. Adv.* **2021**, *2*, 2892–2905. DOI: 10.1039/D1MA00003A.

[31] Li, Y.; Peng, Z.; Holl, N. J.; Hassan, M. R.; Pappas, J. M.; Wei, C.; Izadi, O. H.; Wang, Y.; Dong, X.; Wang, C.; et al. MXene-Graphene Field-Effect Transistor Sensing of Influenza Virus and SARS-CoV-2. *ACS Omega.* **2021**, *6*, 6643–6653. 10.1021/acsomega.0c05421.

[32] Kumar, S.; Lei, Y.; Alshareef, N. H.; Quevedo-Lopez, M. A.; Salama, K. N. Biofunctionalized Two-Dimensional Ti3C2 MXenes for Ultrasensitive Detection of Cancer Biomarker. *Biosens. Bioelectron.* **2018**, *121*, 243–249. 10.1016/j.bios.2018.08.076.

[33] Sadiq, M.; Pang, L.; Johnson, M.; Sathish, V.; Zhang, Q.; Wang, D. 2D Nanomaterial, Ti_3C_2 MXene-Based Sensor to Guide Lung Cancer Therapy and Management. *Biosensors.* **2021**, *11*, 40. DOI: 10.3390/bios11020040.

[34] Zhang, S.; Bilal, M.; Adeel, M.; Barceló, D.; Iqbal, H. M. N. MXene-Based Designer Nanomaterials and Their Exploitation to Mitigate Hazardous Pollutants from Environmental Matrices. *Chemosphere.* **2021**, *283*, 131293. 10.1016/j.chemosphere.2021.131293.

[35] Zhang, X.; Gu, Y. Preparation and Electrochemical Properties of MXene Based Conductive Composites for Food Contamination Detection. *J. Phys.: Conf. Ser.* **2021**, *2076*, 012120. DOI: 10.1088/1742-6596/2076/1/012120.

[36] Sangu, S. S.; Illias, N. M.; Ong, C. C.; Gopinath, S. C. B.; Saheed, M. S. M. MXene-Based Aptasensor: Characterization and High-Performance Voltammetry Detection of Deoxynivalenol. *BioNanoSci.* **2021**, *11*, 314–323. DOI: 10.1007/s12668-021-00847-0.

[37] Kalambate, P. K.; Gadhari, N. S.; Li, X.; Rao, Z.; Navale, S. T.; Shen, Y.; Patil, V. R.; Huang, Y. Recent Advances in MXene–Based Electrochemical Sensors and Biosensors. *TrAC - Trends Anal. Chem.* **2019**, *120*, 115643. DOI: 10.1016/j.trac.2019.115643.

[38] Naguib, M.; Kurtoglu, M.; Presser, V.; Lu, J.; Niu, J.; Heon, M.; Hultman, L.; Gogotsi, Y.; Barsoum, M. W. Two-Dimensional Nanocrystals Produced by Exfoliation of Ti_3AlC_2. *Adv. Mater.* **2011**, *23*, 4248–4253. 10.1002/adma.201102306.

[39] Sang, X.; Xie, Y.; Lin, M. W.; Alhabeb, M.; Van Aken, K. L.; Gogotsi, Y.; Kent, P. R. C.; Xiao, K.; Unocic, R. R. Atomic Defects in Monolayer Titanium Carbide ($Ti_3C_2T_x$) MXene. *ACS Nano.* **2016**, *10*, 9193–9200. 10.1021/acsnano.6b05240.

[40] Ghidiu, M.; Lukatskaya, M. R.; Zhao, M. Q.; Gogotsi, Y.; Barsoum, M. W. Conductive Two-Dimensional Titanium Carbide "Clay" with High Volumetric Capacitance. *Nature.* **2014**, *516*, 78–81. 10.1038/nature13970.

[41] Wang, X.; Garnero, C.; Rochard, G.; Magne, D.; Morisset, S.; Hurand, S.; Chartier, P.; Rousseau, J.; Cabioc'h, T.; Coutanceau, C.; et al. A New Etching Environment (FeF_3/HCl) for the Synthesis of Two-Dimensional Titanium Carbide MXenes: A Route towards Selective Reactivity: Vs. water. *J. Mater. Chem. A.* **2017**, *5*, 22012–22023. DOI: 10.1039/C7TA01082F.

[42] Wang, Z. A Review on MXene: Synthesis, Properties and Applications on Alkali Metal Ion Batteries. *IOP Conf. Ser.: Earth Environ. Sci.* **2021**, *714*, 042030. DOI: 10.1088/1755-1315/714/4/042030.

[43] Halim, J.; Lukatskaya, M. R.; Cook, K. M.; Lu, J.; Smith, C. R.; Näslund, L. Å.; May, S. J.; Hultman, L.; Gogotsi, Y.; Eklund, P.; Barsoum, M. W. Transparent Conductive Two-Dimensional Titanium Carbide Epitaxial Thin Films. *Chem. Mater.* **2014**, *26*, 2374–2381. 10.1021/cm500641a.

[44] Urbankowski, P.; Anasori, B.; Makaryan, T.; Er, D.; Kota, S.; Walsh, P. L.; Zhao, M.; Shenoy, V. B.; Barsoum, M. W.; Gogotsi, Y. Synthesis of Two-Dimensional Titanium Nitride Ti_4N_3 (MXene). *Nanoscale.* **2016**, *8*, 11385–11391. 10.1039/c6nr02253g.

[45] Yang, S.; Zhang, P.; Wang, F.; Ricciardulli, A. G.; Lohe, M. R.; Blom, P. W. M.; Feng, X. Fluoride-Free Synthesis of Two-Dimensional Titanium Carbide (MXene) Using a Binary

Aqueous System. *Angew. Chem. Int. Ed. Engl.* **2018**, *57*, 15491–15495. 10.1002/anie.201809662.

[46] Li, T.; Yao, L.; Liu, Q.; Gu, J.; Luo, R.; Li, J.; Yan, X.; Wang, W.; Liu, P.; Chen, B.; et al. Fluorine-Free Synthesis of High-Purity $Ti_3C_2T_x$ (T = OH, O) via Alkali Treatment. *Angew. Chem. Int. Ed. Engl.* **2018**, *57*, 6115–6119. 10.1002/anie.201800887.

[47] Xuan, J.; Wang, Z.; Chen, Y.; Liang, D.; Cheng, L.; Yang, X.; Liu, Z.; Ma, R.; Sasaki, T.; Geng, F. Organic-Base-Driven Intercalation and Delamination for the Production of Functionalized Titanium Carbide Nanosheets with Superior Photothermal Therapeutic Performance. *Angew. Chem.* **2016**, *128*, 14789–14794. DOI: 10.1002/ange.201606643.

[48] Alhabeb, M.; Maleski, K.; Mathis, T. S.; Sarycheva, A.; Hatter, C. B.; Uzun, S.; Levitt, A.; Gogotsi, Y. Selective Etching of Silicon from Ti3SiC2 (MAX) to Obtain 2D Titanium Carbide (MXene). *Angew. Chem. Int. Ed. Engl.* **2018**, *57*, 5444–5448. 10.1002/anie.201802232.

[49] Lorencova, L.; Bertok, T.; Dosekova, E.; Holazova, A.; Paprckova, D.; Vikartovska, A.; Sasinkova, V.; Filip, J.; Kasak, P.; Jerigova, M.; et al. Electrochemical Performance of $Ti_3C_2T_x$ MXene in Aqueous Media: Towards Ultrasensitive H_2O_2 Sensing. *Electrochim. Acta.* **2017**, *235*, 471–479. 10.1016/j.electacta.2017.03.073.

[50] Lorencova, L.; Gajdosova, V.; Hroncekova, S.; Bertok, T.; Blahutova, J.; Vikartovska, A.; Parrakova, L.; Gemeiner, P.; Kasak, P.; Tkac, J. 2D MXenes as Perspective Immobilization Platforms for Design of Electrochemical Nanobiosensors. *Electroanalysis.* **2019**, *31*, 1833–1844. DOI: 10.1002/elan.201900288.

[51] Xia, T.; Liu, G.; Wang, J.; Hou, S.; Hou, S. MXene-Based Enzymatic Sensor for Highly Sensitive and Selective Detection of Cholesterol. *Biosens. Bioelectron.* **2021**, *183*, 113243. 10.1016/j.bios.2021.113243.

[52] Koyappayil, A.; Chavan, S. G.; Mohammadniaei, M.; Go, A.; Hwang, S. Y.; Lee, M. H. β-Hydroxybutyrate Dehydrogenase Decorated MXene Nanosheets for the Amperometric Determination of β-Hydroxybutyrate. *Microchim. Acta.* **2020**, 187*(5),* 1–7. DOI: 10.1007/s00604-020-04258-y.

[53] Yu, Z.; Jiang, L.; Liu, R.; Zhao, W.; Yang, Z.; Zhang, J.; Jin, S. Versatile Self-Assembled MXene-Au Nanocomposites for SERS Detection of Bacteria, Antibacterial and Photothermal Sterilization. *Chem. Eng. J.* **2021**, *426*, 131914. DOI: 10.1016/j.cej.2021.131914.

[54] Kumar, S.; Singh, R. Recent Optical Sensing Technologies for the Detection of Various Biomolecules: Review. *Opt. Laser Technol.* **2021**, *134*, 106620. DOI: 10.1016/j.optlastec.2020.106620.

[55] Zhang, H. C.; Guo, Y. M. Advances of Carbon Quantum Dots for Fluorescence Turn-On Detection of Reductive Small Biomolecules. *Chin. J. Anal. Chem.* **2021**, *49*, 14–23. DOI: 10.1016/S1872-2040(20)60070-6.

[56] Allen, S. A.; Rednour, S.; Shepard, S.; Pond, B. B. A Simple and Sensitive High-Performance Liquid Chromatography–Electrochemical Detection Assay for the Quantitative Determination of Monoamines and Respective Metabolites in Six Discrete Brain Regions of Mice. *Biomed. Chromatogr.* **2017**, *31*. DOI: 10.1002/bmc.3998.

[57] Li, J.; Tan, S. N.; Ge, H. Silica Sol-Gel Immobilized Amperometric Biosensor for Hydrogen Peroxide. *Anal. Chim. Acta.* **1996**, *335*, 137–145. DOI: 10.1016/S0003-2670(96)00337-6.

[58] Chitra, J.; Ghosh, M.; Mishra, H. N. Rapid Quantification of Cholesterol in Dairy Powders Using Fourier Transform near Infrared Spectroscopy and Chemometrics. *Food Control.* **2017**, *78*, 342–349. DOI: 10.1016/j.foodcont.2016.10.008.

[59] Zhao, M.; Li, Y.; Ma, X.; Xia, M.; Zhang, Y. Adsorption of Cholesterol Oxidase and Entrapment of Horseradish Peroxidase in Metal-Organic Frameworks for the Colorimetric Biosensing of Cholesterol. *Talanta.* **2019**, *200*, 293–299. 10.1016/j.talanta.2019.03.060.

[60] Khan, M. Z. H.; Hasan, M. R.; Hossain, S. I.; Ahommed, M. S.; Daizy, M. Ultrasensitive Detection of Pathogenic Viruses with Electrochemical Biosensor: State of the Art. *Biosens. Bioelectron.* **2020**, *166*, 112431. 10.1016/j.bios.2020.112431.

[61] Li, F.; Ni, B.; Zheng, Y.; Huang, Y.; Li, G. A Simple and Efficient Voltammetric Sensor for Dopamine Determination Based on ZnO Nanorods/Electro-Reduced Graphene Oxide Composite. *Surf. Interfaces.* **2021**, *26*, 101375. DOI: 10.1016/j.surfin.2021.101375.

[62] Li, Q.; Wu, J. T.; Liu, Y.; Qi, X. M.; Jin, H. G.; Yang, C.; Liu, J.; Li, G. L.; He, Q. G. Recent Advances in Black Phosphorus-Based Electrochemical Sensors: A Review. *Anal. Chim. Acta.* **2021**, *1170*, 338480. 10.1016/j.aca.2021.338480.

[63] Li, Q.; Xia, Y.; Wan, X.; Yang, S.; Cai, Z.; Ye, Y.; Li, G. Morphology-Dependent MnO_2/Nitrogen-Doped Graphene Nanocomposites for Simultaneous Detection of Trace Dopamine and Uric Acid. *Mater. Sci. Eng. C Mater. Biol. Appl.* **2020**, *109*, 110615. 10.1016/j.msec.2019.110615.

[64] Liu, H.; Xiong, R.; Zhong, P.; Li, G.; Liu, J.; Wu, J.; Liu, Y.; He, Q. Nanohybrids of Shuttle-like α-Fe_2O_3 nanoparticles and Nitrogen-Doped Graphene for Simultaneous Voltammetric Detection of Dopamine and Uric Acid. *New J. Chem.* **2020**, *44*, 20797–20805. DOI: 10.1039/D0NJ04629A.

[65] Rakhi, R. B.; Nayuk, P.; Xia, C.; Alshareef, H. N. Novel Amperometric Glucose Biosensor Based on MXene Nanocomposite. *Sci. Rep.* **2016**, *6*, 1–9. DOI: 10.1038/srep36422.

[66] Sun, Y.; Li, P.; Zhu, Y.; Zhu, X.; Zhang, Y.; Liu, M.; Liu, Y. In Situ Growth of TiO_2 Nanowires on Ti_3C_2 MXenes Nanosheets as Highly Sensitive Luminol Electrochemiluminescent Nanoplatform for Glucose Detection in Fruits, Sweat and Serum Samples. *Biosens. Bioelectron.* **2021**, *194*, 113600. 10.1016/j.bios.2021.113600.

[67] Li, Z.; Guo, Y.; Yue, H.; Gao, X.; Huang, S.; Zhang, X.; Yu, Y.; Zhang, H.; Zhang, H. Electrochemical Determination of Epinephrine Based on $Ti_3C_2T_x$ MXene-Reduced Graphene Oxide/ITO Electrode. *J. Electroanal. Chem.* **2021**, *895*, 115425. DOI: 10.1016/j.jelechem.2021.115425.

[68] Shahzad, F.; Iqbal, A.; Zaidi, S. A.; Hwang, S. W.; Koo, C. M. Nafion-Stabilized Two-Dimensional Transition Metal Carbide ($Ti_3C_2T_x$ MXene) as a High-Performance Electrochemical Sensor for Neurotransmitter. *J. Ind. Eng. Chem.* **2019**, *79*, 338–344. DOI: 10.1016/j.jiec.2019.03.061.

[69] Zheng, J.; Wang, B.; Ding, A.; Weng, B.; Chen, J. Synthesis of MXene/DNA/Pd/Pt Nanocomposite for Sensitive Detection of Dopamine. *J. Electroanal. Chem.* **2018**, *816*, 189–194. DOI: 10.1016/j.jelechem.2018.03.056.

[70] Liu, J.; Fan, Y.; Chen, G.; Liu, Y. Highly Sensitive Glutamate Biosensor Based on Platinum Nanoparticles Decorated MXene-$Ti_3C_2T_x$ for L-Glutamate Determination in Foodstuffs. *LWT.* **2021**, *148*, 111748. DOI: 10.1016/j.lwt.2021.111748.

[71] Neampet, S.; Ruecha, N.; Qin, J.; Wonsawat, W.; Chailapakul, O.; Rodthongkum, N. A Nanocomposite Prepared from Platinum Particles, Polyaniline and a Ti_3C_2 MXene for Amperometric Sensing of Hydrogen Peroxide and Lactate. *Microchim. Acta.* **2019**, *186(12), 1-8.* DOI: 10.1007/s00604-019-3845-3.

[72] Kaya, H. O.; Cetin, A. E.; Azimzadeh, M.; Topkaya, S. N. Pathogen Detection with Electrochemical Biosensors: Advantages, Challenges and Future Perspectives. *J. Electroanal. Chem. (Lausanne).* **2021**, *882*, 114989. 10.1016/j.jelechem.2021.114989.

[73] Vermisoglou, E.; Panáček, D.; Jayaramulu, K.; Pykal, M.; Frébort, I.; Kolář, M.; Hajdúch, M.; Zbořil, R.; Otyepka, M. Human Virus Detection with Graphene-Based Materials. *Biosens. Bioelectron.* **2020**, *166*, 112436. 10.1016/j.bios.2020.112436.

[74] Bacchu, M. S.; Ali, M. R.; Das, S.; Akter, S.; Sakamoto, H.; Suye, S. I.; Rahman, M. M.; Campbell, K.; Khan, M. Z. H. A DNA Functionalized Advanced Electrochemical Biosensor for Identification of the Foodborne Pathogen Salmonella enterica Serovar Typhi in Real Samples. *Anal. Chim. Acta.* **2022**, *1192*, 339332. DOI: 10.1016/j.aca.2021.339332.

[75] Ji, T.; Liu, Z.; Wang, G. Q.; Guo, X.; Akbar khan, S.; Lai, C.; Chen, H.; Huang, S.; Xia, S.; Chen, B.; et al. Detection of COVID-19: A Review of the Current Literature and Future Perspectives. *Biosens. Bioelectron.* **2020**, *166*, 112455. 10.1016/j.bios.2020.112455.

[76] Chowdhury, A. D.; Takemura, K.; Li, T. C.; Suzuki, T.; Park, E. Y. Electrical Pulse-Induced Electrochemical Biosensor for Hepatitis E Virus Detection. *Nat. Commun.* **2019**, *10*, 4–7. DOI: 10.1038/s41467-019-11644-5.

[77] Váradi, L.; Luo, J. L.; Hibbs, D. E.; Perry, J. D.; Anderson, R. J.; Orenga, S.; Groundwater, P. W. Methods for the Detection and Identification of Pathogenic Bacteria: Past, Present, and Future. *Chem. Soc. Rev.* **2017**, *46*, 4818–4832. 10.1039/c6cs00693k.

[78] Wan, Y.; Zhu, G. Dopamine-Mediated Immunoassay for Bacteria Detection. *Anal. Bioanal. Chem.* **2017**, *409*, 6091–6096. 10.1007/s00216-017-0545-x.

[79] Maartens, G.; Griesel, R.; Dube, F.; Nicol, M.; Mendelson, M. Etiology of Pulmonary Infections in Human Immunodeficiency Virus-Infected Inpatients Using Sputum Multiplex Real-Time Polymerase Chain Reaction. *Clin. Infect. Dis.* **2020**, *70*, 1147–1152. 10.1093/cid/ciz332.

[80] Li, G.; Qi, X.; Wu, J.; Xu, L.; Wan, X.; Liu, Y.; Chen, Y.; Li, Q. Ultrasensitive, Label-Free Voltammetric Determination of Norfloxacin Based on Molecularly Imprinted Polymers and Au Nanoparticle-Functionalized Black Phosphorus Nanosheet Nanocomposite. *J. Hazard. Mater.* **2022a**, *436*, 129107. 10.1016/j.jhazmat.2022.129107.

[81] Li, G.; Qi, X.; Zhang, G.; Wang, S.; Li, K.; Wu, J.; Wan, X.; Liu, Y.; Li, Q. Low-Cost Voltammetric Sensors for Robust Determination of Toxic Cd(II) and Pb(II) in Environment and Food Based on Shuttle-like α-Fe_2O_3 Nanoparticles Decorated β-Bi_2O_3 Microspheres. *Microchem. J.* **2022b**, *179*, 107515. DOI: 10.1016/j.microc.2022.107515.

[82] Li, G.; Wu, J.; Qi, X.; Wan, X.; Liu, Y.; Chen, Y.; Xu, L. Molecularly Imprinted Polypyrrole Film-Coated Poly(3,4-Ethylenedioxythiophene): Polystyrene Sulfonate-Functionalized Black Phosphorene for the Selective and Robust Detection of Norfloxacin. *Mater. Today Chem.* **2022c**, *26*, 101043. DOI: 10.1016/j.mtchem.2022.101043.

[83] Hantanasirisakul, K.; Gogotsi, Y. Electronic and Optical Properties of 2D Transition Metal Carbides and Nitrides (MXenes). *Adv. Mater.* **2018**, *30*, 1804779. DOI: 10.1002/adma.201804779.

[84] Wei, W.; Lin, H.; Hao, T.; Su, X.; Jiang, X.; Wang, S.; Hu, Y.; Guo, Z. Dual-Mode ECL/SERS Immunoassay for Ultrasensitive Determination of Vibrio vulnificus Based on Multifunctional MXene. *Sens. Actuators, B Chem.* **2021**, *332*, 129525. DOI: 10.1016/j.snb.2021.129525.

[85] Chen, R.; Kan, L.; Duan, F.; He, L.; Wang, M.; Cui, J.; Zhang, Z.; Zhang, Z. Surface Plasmon Resonance Aptasensor Based on Niobium Carbide MXene Quantum Dots for Nucleocapsid of SARS-CoV-2 Detection. *Microchim. Acta.* **2021**, *188(10), 1-10*. DOI: 10.1007/s00604-021-04974-z.

[86] Wang, Y.; Sun, W.; Li, Y.; Zhuang, X.; Tian, C.; Luan, F.; Fu, X. Imidazole Metal-Organic Frameworks Embedded in Layered $Ti_3C_2T_x$ Mxene as a High-Performance Electrochemiluminescence Biosensor for Sensitive Detection of HIV-1 Protein. *Microchem. J.* **2021**, *167*, 106332. DOI: 10.1016/j.microc.2021.106332.

[87] Peng, X.; Zhang, Y.; Lu, D.; Guo, Y.; Guo, S. Ultrathin Ti_3C_2 Nanosheets Based "off-on" Fluorescent Nanoprobe for Rapid and Sensitive Detection of HPV Infection. *Sens. Actuators, B Chem.* **2019**, *286*, 222–229. DOI: 10.1016/j.snb.2019.01.158.

[88] Zhang, J.; Li, Y.; Duan, S.; He, F. Highly Electrically Conductive Two-Dimensional Ti_3C_2 Mxenes-Based 16S rDNA Electrochemical Sensor for Detecting Mycobacterium Tuberculosis. *Anal. Chim. Acta.* **2020**, *1123*, 9–17. 10.1016/j.aca.2020.05.013.

[89] Wang, L.; Cui, K.; Wang, P.; Pei, M.; Guo, W. A Sensitive Electrochemical DNA Sensor for Detecting Helicobacter pylori Based on Accordion-like $Ti_3C_2T_x$: A Simple Strategy. *Anal. Bioanal. Chem.* **2021**, *413*(16), 4353-4362.. DOI: 10.1007/s00216-021-03391-8.

[90] Hasan, M. R.; Ahommed, M. S.; Daizy, M.; Bacchu, M. S.; Ali, M. R.; Al-Mamun, M. R.; Saad Aly, M. A.; Khan, M. Z. H.; Hossain, S. I. Recent Development in Electrochemical Biosensors for Cancer Biomarkers Detection. *Biosens. Bioelectron.* **2021**, *8*, 100075. DOI: 10.1016/j.biosx.2021.100075.

[91] Yang, X.; Feng, M.; Xia, J.; Zhang, F.; Wang, Z. An Electrochemical Biosensor Based on AuNPs/Ti_3C_2 MXene Three-Dimensional Nanocomposite for microRNA-155 Detection by Exonuclease III-Aided Cascade Target Recycling. *J. Electroanal. Chem.* **2020**, *878*, 114669. DOI: 10.1016/j.jelechem.2020.114669.

[92] Xu, B.; Zhu, M.; Zhang, W.; Zhen, X.; Pei, Z.; Xue, Q.; Zhi, C.; Shi, P. Ultrathin MXene-Micropattern-Based Field-Effect Transistor for Probing Neural Activity. *Adv. Mater.* **2016**, *28*, 3333–3339. 10.1002/adma.201504657.

[93] Medetalibeyoglu, H.; Kotan, G.; Atar, N.; Yola, M. L. A Novel Sandwich-Type SERS Immunosensor for Selective and Sensitive Carcinoembryonic Antigen (CEA) Detection. *Anal. Chim. Acta.* **2020a**, *1139*, 100–110. 10.1016/j.aca.2020.09.034.

[94] Wu, Q.; Li, N.; Wang, Y.; Xu, Y.; Wu, J.; Jia, G.; Ji, F.; Fang, X.; Chen, F.; Cui, X. Ultrasensitive and Selective Determination of Carcinoembryonic Antigen Using Multifunctional Ultrathin Amino-Functionalized Ti_3C_2-MXene Nanosheets. *Anal. Chem.* **2020**, *92*, 3354–3360. 10.1021/acs.analchem.9b05372.

[95] Sharifuzzaman, M.; Barman, S. C.; Zahed, M. A.; Sharma, S.; Yoon, H.; Nah, J. S.; Kim, H.; Park, J. Y. An Electrodeposited MXene-$Ti_3C_2T_x$ Nanosheets Functionalized by Task-Specific Ionic Liquid for Simultaneous and Multiplexed Detection of Bladder Cancer Biomarkers. *Small.* **2020**, *16*, 2002517. DOI: 10.1002/smll.202002517.

[96] Medetalibeyoglu, H.; Kotan, G.; Atar, N.; Yola, M. L. A Novel and Ultrasensitive Sandwich-Type Electrochemical Immunosensor Based on Delaminated MXene@AuNPs as Signal Amplification for Prostate Specific Antigen (PSA) Detection and Immunosensor Validation. *Talanta.* **2020b**, *220*, 121403. 10.1016/j.talanta.2020.121403.

[97] Wu, Q.; Li, N.; Wang, Y.; Liu, Y.; Xu, Y.; Wei, S.; Wu, J.; Jia, G.; Fang, X.; Chen, F.; Cui, X. A 2D Transition Metal Carbide MXene-Based SPR Biosensor for Ultrasensitive Carcinoembryonic Antigen Detection. *Biosens. Bioelectron.* **2019**, *144*, 111697. 10.1016/j.bios.2019.111697.

[98] Wang, Y.; Zeng, S.; Crunteanu, A.; Xie, Z.; Humbert, G.; Ma, L.; Wei, Y.; Brunel, A.; Bessette, B.; Orlianges, J. C.; et al. Targeted Sub-Attomole Cancer Biomarker Detection Based on Phase Singularity 2D Nanomaterial-Enhanced Plasmonic Biosensor. *Nano-Micro Lett.* **2021**, *13*, 11. DOI: 10.1007/s40820-021-00613-7.

[99] Cheng, J.; Hu, K.; Liu, Q.; Liu, Y.; Yang, H.; Kong, J. Electrochemical Ultrasensitive Detection of CYFRA21-1 Using $Ti_3C_2T_x$-MXene as Enhancer and Covalent Organic Frameworks as Labels. *Anal. Bioanal. Chem.* **2021**, *413*, 2543–2551. 10.1007/s00216-021-03212-y.

[100] Zhang, C.; Jiang, C.; Lan, L.; Ping, J.; Ye, Z.; Ying, Y. Nanomaterial-Based Biosensors for Agro-Product Safety. *TrAC - Trends Anal. Chem.* **2021**, *143*, 116369. DOI: 10.1016/j.trac.2021.116369.

[101] Tian, L.; Qi, J.; Ma, X.; Wang, X.; Yao, C.; Song, W.; Wang, Y. A Facile DNA Strand Displacement Reaction Sensing Strategy of Electrochemical Biosensor Based on N-Carboxymethyl

Chitosan/Molybdenum Carbide Nanocomposite for microRNA-21 Detection. *Biosens. Bioelectron.* **2018**, *122*, 43–50. 10.1016/j.bios.2018.09.037.

[102] Wang, H.; Sun, J.; Lu, L.; Yang, X.; Xia, J.; Zhang, F.; Wang, Z. Competitive Electrochemical Aptasensor Based on a cDNA-Ferrocene/MXene Probe for Detection of Breast Cancer Marker Mucin1. *Anal. Chim. Acta.* **2020**, *1094*, 18–25. 10.1016/j.aca.2019.10.003.

[103] Hroncekova, S.; Bertok, T.; Hires, M.; Jane, E.; Lorencova, L.; Vikartovska, A.; Tanvir, A.; Kasak, P.; Tkac, J. Ultrasensitive $Ti_3C_2T_X$ MXene/Chitosan Nanocomposite-Based Amperometric Biosensor for Detection of Potential Prostate Cancer Marker in Urine Samples. *Processes (Basel).* **2020**, *8*, 580. 10.3390/PR8050580.

[104] Nagarajan, R. D.; Murugan, P.; Palaniyandi, K.; Atchudan, R.; Sundramoorthy, A. K. Biocompatible MXene ($Ti_3C_2T_x$) Immobilized with Flavin Adenine Dinucleotide as an Electrochemical Transducer for Hydrogen Peroxide Detection in Ovarian Cancer Cell Lines. *Micromachines.* **2021**, *12*, 862. DOI: 10.3390/mi12080862.

[105] Zhang, M.; Mei, L.; Zhang, L.; Wang, X.; Liao, X.; Qiao, X.; Hong, C. Ti_3C_2 MXene Anchors CuAu-LDH Multifunctional Two-Dimensional Nanomaterials for Dual-Mode Detection of CEA in Electrochemical Immunosensors. *Bioelectrochemistry.* **2021**, *142*, 107943. 10.1016/j.bioelechem.2021.107943.

[106] Rizzo, D. M.; Lichtveld, M.; Mazet, J. A. K.; Togami, E.; Miller, S. A. Plant Health and Its Effects on Food Safety and Security in a One Health Framework: Four Case Studies. *One Heal. Outlook.* **2021**, *3(1), 1-9.*. DOI: 10.1186/s42522-021-00038-7.

[107] Bennett, J. W.; Klich, M.; Mycotoxins, M. Mycotoxins. *Clin. Microbiol. Rev.* **2003**, *16*, 497–516. 10.1128/CMR.16.3.497.

[108] Omotayo, O. P.; Omotayo, A. O.; Mwanza, M.; Babalola, O. O. Prevalence of Mycotoxins and Their Consequences on Human Health. *Toxicol. Res.* **2019**, *35*, 1–7. 10.5487/TR.2019.35.1.001.

[109] Goud, K. Y.; Kailasa, S. K.; Kumar, V.; Tsang, Y. F.; Lee, S. E.; Gobi, K. V.; Kim, K.-H. Progress on Nanostructured Electrochemical Sensors and Their Recognition Elements for Detection of Mycotoxins: A Review. *Biosens. Bioelectron.* **2018**, *121*, 205–222. 10.1016/j.bios.2018.08.029.

[110] Wang, H.; Li, H.; Huang, Y.; Xiong, M.; Wang, F.; Li, C. A Label-Free Electrochemical Biosensor for Highly Sensitive Detection of Gliotoxin Based on DNA Nanostructure/MXene Nanocomplexes. *Biosens. Bioelectron.* **2019**, *142*, 111531. 10.1016/j.bios.2019.111531.

[111] Zhang, D.; Pu, H.; Huang, L.; Sun, D. W. Advances in Flexible Surface-Enhanced Raman Scattering (SERS) Substrates for Nondestructive Food Detection: Fundamentals and Recent Applications. *Trends Food Sci. Technol.* **2021**, *109*, 690–701. DOI: 10.1016/j.tifs.2021.01.058.

[112] Zhu, X.; Chen, H.; Zhou, Y.; Wu, J.; Ramakrishna, S.; Peng, X.; Nanda, H. S.; Zhou, Y. Recent Advances in Biosensors for Detection of Exosomes. *Curr. Opin. Biomed. Eng.* **2021**, *18*, 100280. DOI: 10.1016/j.cobme.2021.100280.

[113] Wu, Z.; Sun, D. W.; Pu, H.; Wei, Q.; Lin, X. $Ti_3C_2T_x$ MXenes Loaded with Au Nanoparticle Dimers as a Surface-Enhanced Raman Scattering Aptasensor for AFB1 Detection. *Food Chem.* **2022**, *372*, 131293. 10.1016/j.foodchem.2021.131293.

[114] Lawson, B.; Robinson, R. A.; Parmar, M.; Killick, R.; Cunningham, A. A.; MacDonald, S. J. Aflatoxin and Ochratoxin a Residues in Supplementary Foods Used for Wild Birds. *Sci. Total Environ.* **2020**, *731*, 138851. 10.1016/j.scitotenv.2020.138851.

[115] Zheng, F.; Ke, W.; Shi, L.; Liu, H.; Zhao, Y. Plasmonic Au-Ag Janus Nanoparticle Engineered Ratiometric Surface-Enhanced Raman Scattering Aptasensor for Ochratoxin a Detection. *Anal. Chem.* **2019**, *91*, 11812–11820. 10.1021/acs.analchem.9b02469.

[116] Jiang, C.; Lan, L.; Yao, Y.; Zhao, F.; Ping, J. Recent Progress in Application of Nanomaterial-Enabled Biosensors for Ochratoxin a Detection. *TrAC - Trends Anal. Chem.* **2018**, *102*, 236–249. DOI: 10.1016/j.trac.2018.02.007.

[117] He, D.; Wu, Z.; Cui, B.; Xu, E.; Jin, Z. Building a Fluorescent Aptasensor Based on Exonuclease-Assisted Target Recycling Strategy for One-Step Detection of T-2 Toxin. *Food Anal. Methods.* **2019**, *12*, 625–632. DOI: 10.1007/s12161-018-1392-x.

[118] Bai, S. H.; Ogbourne, S. M. Glyphosate: Environmental Contamination, Toxicity and Potential Risks to Human Health via Food Contamination. *Environ. Sci. Pollut. Res. Int.* **2016**, *23*, 18988–19001. 10.1007/s11356-016-7425-3.

[119] Eze, I. C.; Schaffner, E.; Fischer, E.; Schikowski, T.; Adam, M.; Imboden, M.; Tsai, M.; Carballo, D.; von Eckardstein, A.; Künzli, N.; et al. Long-Term Air Pollution Exposure and Diabetes in a Population-Based Swiss Cohort. *Environ. Int.* **2014**, *70*, 95–105. DOI: 10.1016/j.envint.2014.05.014.

[120] Kelishadi, R.; Poursafa, P. Air Pollution and Non-Respiratory Health Hazards for Children. *Arch. Med. Sci.* **2010**, *6*, 483–495. 10.5114/aoms.2010.14458.

[121] Kuppala, G. Ecological and Health Impacts of Air Pollution. Journal of Environmental Hazards **2021**, *5*, 5–6.

[122] Manisalidis, I.; Stavropoulou, E.; Stavropoulos, A.; Bezirtzoglou, E. Environmental and Health Impacts of Air Pollution: A Review. *Front. Public Heal.* **2020**, *8*, 1–13. DOI: 10.3389/fpubh.2020.00014.

[123] Simpson, M. J. Global Climate Change Impacts in the United States. *J. Environ. Qual.* **2011**, *40*, 279–279. DOI: 10.2134/jeq2010.0010br.

[124] Erxleben, H.; Ruzicka, J. Atomic Absorption Spectroscopy for Mercury, Automated by Sequential Injection and Miniaturized in Lab-on-Valve System. *Anal. Chem.* **2005**, *77*, 5124–5128. 10.1021/ac058007s.

[125] Li, Y.; Chen, C.; Li, B.; Sun, J.; Wang, J.; Gao, Y.; Zhao, Y.; Chai, Z. Elimination Efficiency of Different Reagents for the Memory Effect of Mercury Using ICP-MS. *J. Anal. At. Spectrom.* **2006**, *21*, 94–96. DOI: 10.1039/B511367A.

[126] Zhu, Z.; Chan, G. C.-Y.; Ray, S. J.; Zhang, X.; Hieftje, G. M. Use of a Solution Cathode Glow Discharge for Cold Vapor Generation of Mercury with Determination by ICP-Atomic Emission Spectrometry. *Anal. Chem.* **2008**, *80*, 7043–7050. 10.1021/ac8011126.

[127] Guo, Y.; Zhang, L.; Zhang, S.; Yang, Y.; Chen, X.; Zhang, M. Fluorescent Carbon Nanoparticles for the Fluorescent Detection of Metal Ions. *Biosens. Bioelectron.* **2015**, *63*, 61–71. 10.1016/j.bios.2014.07.018.

[128] Memon, A. G.; Xing, Y.; Zhou, X.; Wang, R.; Liu, L.; Zeng, S.; He, M.; Ma, M. Ultrasensitive Colorimetric Aptasensor for Hg(2+) Detection Using Exo-III Assisted Target Recycling Amplification and Unmodified AuNPs as Indicators. *J. Hazard. Mater.* **2020**, *384*, 120948. 10.1016/j.jhazmat.2019.120948.

[129] Saleh, T. A.; Fadillah, G.; Ciptawati, E.; Khaled, M. Analytical Methods for Mercury Speciation, Detection, and Measurement in Water, Oil, and Gas. *TrAC - Trends Anal. Chem.* **2020**, *132*, 116016. DOI: 10.1016/j.trac.2020.116016.

[130] Van Neste, C. W.; Senesac, L. R.; Thundat, T. Standoff Photoacoustic Spectroscopy. *Appl. Phys. Lett.* **2008**, *92*, 234102. DOI: 10.1063/1.2945288.

[131] Kannan, P. K.; Late, D. J.; Morgan, H.; Rout, C. S. Recent Developments in 2D Layered Inorganic Nanomaterials for Sensing. *Nanoscale.* **2015**, *7*, 13293–13312. 10.1039/C5NR03633J.

[132] Tang, J.; Liu, X.; Yang, C.; Zhang, Z.; Sun, R.; Li, H.; Li, C.; Wang, F. A Carbon-Rich Nanofiber Framework Based on a Conjugated Arylacetylene Polymer for Photocathodic Enzymatic Bioanalysis. *RSC Adv.* **2019**, *9*, 42533–42542. 10.1039/c9ra09157b.

[133] Sun, J. Y.; Huang, K. J.; Zhao, S. F.; Fan, Y.; Wu, Z. W. Direct Electrochemistry and Electrocatalysis of Hemoglobin on Chitosan-Room Temperature Ionic liquid-TiO_2-Graphene

Nanocomposite Film Modified Electrode. *Bioelectrochemistry.* **2011**, *82*, 125–130. 10.1016/j.bioelechem.2011.06.007.

[134] Liu, H.; Duan, C.; Yang, C.; Shen, W.; Wang, F.; Zhu, Z. A Novel Nitrite Biosensor Based on the Direct Electrochemistry of Hemoglobin Immobilized on MXene-Ti_3C_2. *Sens. Actuators B Chem.* **2015**, *218*, 60–66. DOI: 10.1016/j.snb.2015.04.090.

[135] Zhou, L.; Zhang, X.; Ma, L.; Gao, J.; Jiang, Y. Acetylcholinesterase/Chitosan-Transition Metal Carbides Nanocomposites-Based Biosensor for the Organophosphate Pesticides Detection. *Biochem. Eng. J.* **2017**, *128*, 243–249. DOI: 10.1016/j.bej.2017.10.008.

[136] Song, D.; Jiang, X.; Li, Y.; Lu, X.; Luan, S.; Wang, Y.; Li, Y.; Gao, F. Metal – Organic Frameworks-Derived MnO_2/Mn_3O_4 Microcuboids with Hierarchically Ordered Nanosheets and Ti_3C_2 MXene/Au NPs Composites for Electrochemical Pesticide Detection. *J. Hazard. Mater.* **2019**, *373*, 367–376. 10.1016/j.jhazmat.2019.03.083.

[137] Zhao, F.; Yao, Y.; Jiang, C.; Shao, Y.; Barceló, D.; Ying, Y.; Ping, J. Self-Reduction Bimetallic Nanoparticles on Ultrathin MXene Nanosheets as Functional Platform for Pesticide Sensing. *J. Hazard. Mater.* **2020**, *384*, 121358. 10.1016/j.jhazmat.2019.121358.